Please cite this article in press as: Jaehnig et al., Checkpoint Kinases Regulate a Global Network of Transcription Factors in Response to DNA Damage, Cell Reports (2013), http://dx.doi.org/10.1016/j.celrep.2013.05.041

Cell Reports
Resource

Checkpoint Kinases Regulate a Global Network of Transcription Factors in Response to DNA Damage

Eric J. Jaehnig,[1,2,3] Dwight Kuo,[4] Hans Hombauer,[1,2,3] Trey G. Ideker,[2,4,5,6] and Richard D. Kolodner[1,2,3,5,6,*]
[1]Ludwig Institute for Cancer Research, University of California School of Medicine, San Diego, 9500 Gilman Drive, La Jolla, CA 92093, USA
[2]Department of Medicine, University of California School of Medicine, San Diego, 9500 Gilman Drive, La Jolla, CA 92093, USA
[3]Department of Cellular and Molecular Medicine, University of California School of Medicine, San Diego, 9500 Gilman Drive, La Jolla, CA 92093, USA
[4]Department of Bioengineering, University of California School of Medicine, San Diego, 9500 Gilman Drive, La Jolla, CA 92093, USA
[5]UCSD Moores Cancer Center, University of California School of Medicine, San Diego, 9500 Gilman Drive, La Jolla, CA 92093, USA
[6]Institute of Genomic Medicine, University of California School of Medicine, San Diego, 9500 Gilman Drive, La Jolla, CA 92093, USA
*Correspondence: rkolodner@ucsd.edu
http://dx.doi.org/10.1016/j.celrep.2013.05.041

SUMMARY

DNA damage activates checkpoint kinases that induce several downstream events, including widespread changes in transcription. However, the specific connections between the checkpoint kinases and downstream transcription factors (TFs) are not well understood. Here, we integrate kinase mutant expression profiles, transcriptional regulatory interactions, and phosphoproteomics to map kinases and downstream TFs to transcriptional regulatory networks. Specifically, we investigate the role of the *Saccharomyces cerevisiae* checkpoint kinases (Mec1, Tel1, Chk1, Rad53, and Dun1) in the transcriptional response to DNA damage caused by methyl methanesulfonate. The result is a global kinase-TF regulatory network in which Mec1 and Tel1 signal through Rad53 to synergistically regulate the expression of more than 600 genes. This network involves at least nine TFs, many of which have Rad53-dependent phosphorylation sites, as regulators of checkpoint-kinase-dependent genes. We also identify a major DNA damage-induced transcriptional network that regulates stress response genes independently of the checkpoint kinases.

INTRODUCTION

DNA damage can be caused by exogenous agents, such as carcinogens and ionizing radiation, and by endogenous agents, such as reactive oxidative species. This can result in errors during DNA replication or blockage of the replication machinery, leading to mutations or genomic rearrangements. Cellular function or viability may be impaired if the resulting mutations or genomic rearrangements affect critical genes. In addition, alteration of genes with roles in cellular homeostasis, such as control of the cell cycle, cell migration, or cellular adhesion, may contribute to the development of cancer (Branzei and Foiani, 2009; Kolodner et al., 2002).

Response mechanisms that recognize DNA damage are well conserved in eukaryotes. The DNA damage response (DDR) involves a signal transduction cascade in which recognition of DNA damage activates checkpoint kinases from the PI3K-like family, particularly ataxia telangiectasia mutated (ATM) and ATM/Rad3 related (ATR) (Mec1 and Tel1 in *S. cerevisiae*; see Figure 1A). ATM and ATR then phosphorylate Chk family checkpoint kinases, including Chk1 and Chk2 (Chk1 and Rad53 in *S. cerevisiae*; Rad53 also phosphorylates a third checkpoint kinase, Dun1), but the relative importance of each checkpoint kinase to the DDR depends on the type of DNA damage. The activated checkpoint kinases phosphorylate numerous effector proteins that regulate multiple cellular processes, including cell-cycle progression, DNA replication and repair, and, in multicellular organisms, apoptosis (Branzei and Foiani, 2006; Putnam et al., 2009; Rouse and Jackson, 2002).

Activation of the checkpoint kinases also induces changes in expression of hundreds to thousands of genes in *S. cerevisiae* (Gasch et al., 2001; Putnam et al., 2009; Workman et al., 2006). In one example, the transcription factor (TF) Rfx1/Crt1 represses multiple targets, including the ribonucleotide reductase genes (*RNR2*, *RNR3*, and *RNR4*), *HUG1*, and *RFX1* itself (Figure 1A) (Basrai et al., 1999; Huang et al., 1998). Following DNA damage, repression is relieved by hyperphosphorylation of Rfx1 by Dun1 (Huang et al., 1998). Interestingly, most of the genes that are differentially expressed in response to DNA damage are not involved in DNA repair but rather act in other processes such as cell-cycle progression, environmental stress responses, protein homeostasis, and energy metabolism (Gasch et al., 2001; Putnam et al., 2009). For example, Rad53 phosphorylates and potentially represses Swi6, a TF that drives expression of genes that promote cell-cycle progression from G1 to S phase (Sidorova and Breeden, 1997, 2003).

Previously, we used genome-wide chromatin immunoprecipitation (ChIP) and TF mutant expression profiling to map

Please cite this article in press as: Jaehnig et al., Checkpoint Kinases Regulate a Global Network of Transcription Factors in Response to DNA Damage, Cell Reports (2013), http://dx.doi.org/10.1016/j.celrep.2013.05.041

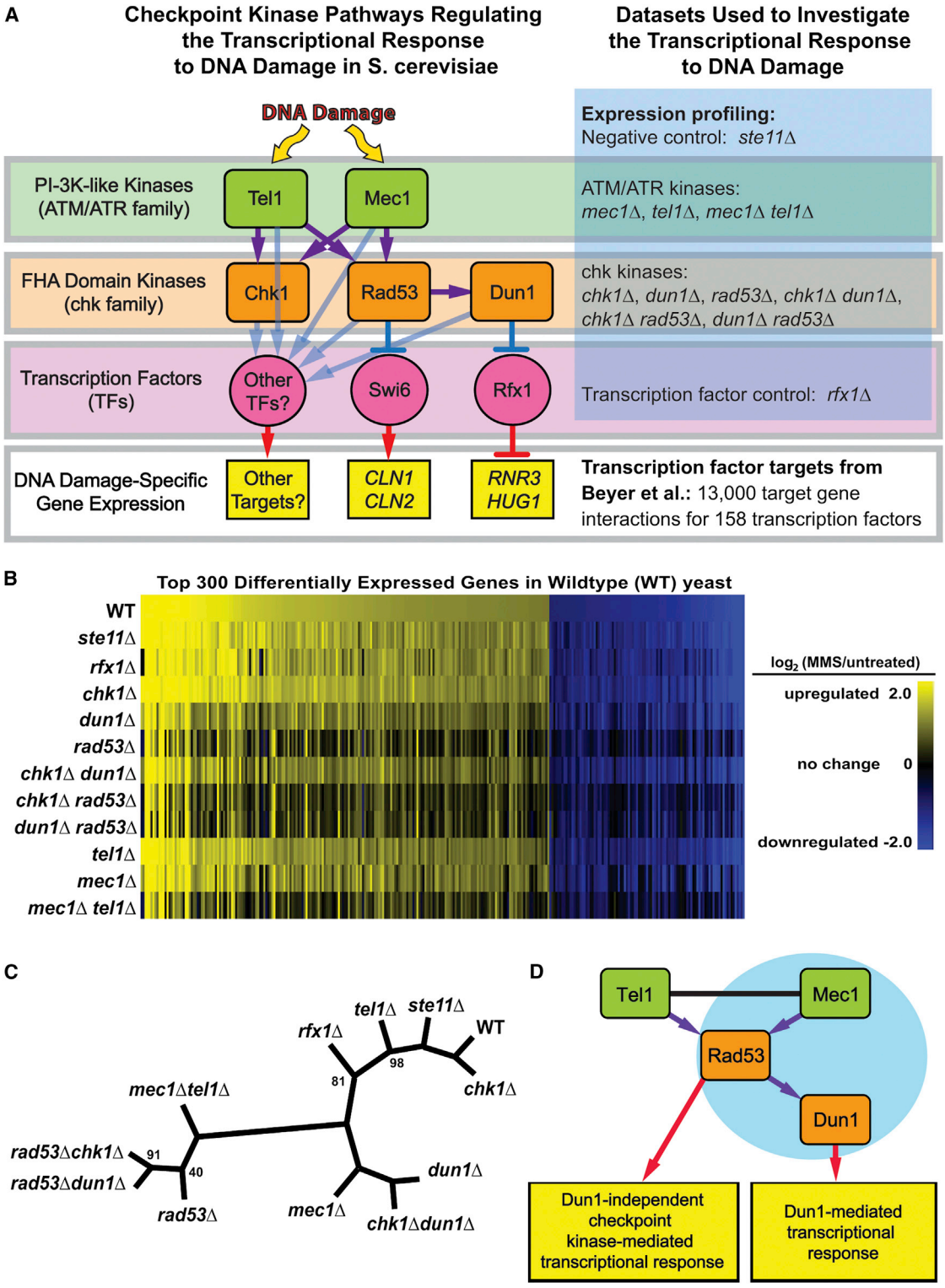

Figure 1. Regulation of the Transcriptional Response to DNA Damage by the Checkpoint Kinase Signaling Cascade

(A) Model for the regulation of transcription by the DNA damage checkpoint kinases (left) and overview of the data sets analyzed (right).

(B) MMS-induced changes in expression for each strain are shown here as vertical bars representing the log ratios (base 2) of gene expression in MMS-treated relative to untreated yeast for each of the 300 most differentially expressed genes in WT. Complete analysis of differential expression is provided in Table S2.

(legend continued on next page)

transcriptional networks underlying the DDR induced by methyl methanesulfonate (MMS) in *S. cerevisiae* (Workman et al., 2006). These data have since been combined with data from other high-throughput studies to identify potential transcriptional targets for most known *S. cerevisiae* TFs (Beyer et al., 2006). Here, we integrate this transcriptional network with gene expression profiles of checkpoint kinase mutants to map interactions between kinases and TFs during the DDR. We further explored kinase-TF interactions using mass spectrometry to identify checkpoint-kinase-dependent phosphorylation sites on candidate TFs. We found that the checkpoint-kinase-mediated transcriptional response is more complex than previously appreciated. Specifically, activation of Rad53 in a manner dependent on Mec1 and, to a greater extent than other MMS-induced checkpoint responses, on Tel1 plays a central role in inducing a transcriptional network that involves both Dun1-dependent and Dun1-independent branches. In addition, we identified transcriptional networks induced by DNA damage independently of the checkpoint kinases.

RESULTS

Rad53 Is the Central Regulator of the Checkpoint-Kinase-Dependent Transcriptional Response to DNA Damage

We analyzed the mRNA expression profiles of *S. cerevisiae* before and after exposure to MMS in wild-type (WT) cells and in checkpoint kinase single and double mutants (strains shown in Figure 1A and Table S1; expression profile data shown in Table S2). Approximately 1,700 genes showed significant expression changes during the DDR in WT cells (Table S3). As shown in Figure 1B, differential expression of a number of genes was attenuated by deletion of *MEC1*, *RAD53*, or *DUN1*. In contrast, deletion of *STE11*, a kinase that mediates the pheromone response during mating (Bardwell, 2004), did not substantially affect DNA damage-induced changes in gene expression (Figure 1B; Table S3).

Hierarchical clustering of the WT and mutant differential expression profiles revealed high-level insights into their regulatory relationships (Figure 1C). In the resulting tree, the distance between two strains reflects the difference between the expression profiles of the strains, and the distance of a strain from WT indicates the severity of its defect in the transcriptional response to MMS (Ideker et al., 2001; Van Driessche et al., 2005). For instance, *chk1Δ* clustered closely with WT, *chk1Δdun1Δ* clustered with *dun1Δ*, and *chk1Δrad53Δ* clustered with *rad53Δ*, suggesting that Chk1 does not contribute significantly to the transcriptional response to MMS. The expression profile of *rad53Δdun1Δ* was similar to that of *rad53Δ* and distinct from that of *dun1Δ*, and the expression profile of the *dun1Δ* mutant was much closer to WT than that of the *rad53Δ* mutant, consistent with Dun1 acting downstream of Rad53 and with a larger fraction of the transcriptional response being mediated by Rad53 than by Dun1 (Figure 1C) (Allen et al., 1994; Bashkirov et al., 2003). The distance between the WT and *mec1Δ* expression profiles confirmed that Mec1 plays an important role in regulating the transcriptional response to MMS (Gasch et al., 2001). A *tel1Δ* mutation resulted in only minor defects in the MMS-induced expression profile. However, the *mec1Δtel1Δ* double mutant affected the transcriptional response to a much greater extent than *mec1Δ*. Finally, the *mec1Δtel1Δ* and *rad53Δ* mutants had differential expression profiles that showed similar defects, supporting the model that Mec1 and Tel1 converge on Rad53 to regulate the checkpoint-kinase-dependent branch of the transcriptional response (Figure 1D).

Implicating Downstream TFs in the Checkpoint-Kinase-Dependent Transcriptional Response

To map the transcriptional network induced by the checkpoint kinases, we first identified the genes whose DNA damage-induced transcriptional response was dependent on each kinase. Figure 2A illustrates this for a subset of genes in the *dun1Δ* experiment: *HUG1* and *RNR3* are targets of the Rfx1 TF, which is regulated by Dun1 (Figure 1A) (Basrai et al., 1999; Huang et al., 1998). Both *HUG1* and *RNR3* were upregulated by MMS in the WT strain but showed a reduced response in the *dun1Δ* mutant (Figure 2A). Similarly, *ADE4* and *HOF1* were downregulated in WT but not in the *dun1Δ* mutant. We refer to these genes as "kinase dependent" because they require the kinase for full differential expression during the DDR.

By evaluating genes for statistically significant reductions in differential expression in each of the kinase mutants (Table S2; Table S4 lists the kinase dependencies and other properties for all genes included in the expression analysis), we identified 109 and 146 genes that were dependent on Dun1 and Mec1, respectively (Figure 2B; Table S3). Many more genes were dependent on Rad53 (~600 genes), providing an estimate for the number of checkpoint-kinase-dependent genes. Consistent with the model in which Dun1 regulates Rfx1, this analysis revealed that 41 genes, including known Rfx1 targets (*FSH3*, *HUG1*, *RNR2*, *RNR3*, and *RNR4*), showed a reduction in differential expression in the *rfx1Δ* mutant and that 16 and 39 of these showed reduced differential expression in *dun1Δ* and *rad53Δ* mutants, respectively (Tables S4 and S5) (Basrai et al., 1999; Huang et al., 1998).

Using a previously defined TF regulatory network comprising approximately 13,000 TF-target gene interactions for 158 TFs (Beyer et al., 2006), we identified TFs whose targets showed significant enrichment for kinase-dependent genes (Figure 3A; Table S6). In these cases, the kinase was inferred to mediate expression of the target genes by regulating the activity of that TF during the DDR. Figure 3B shows the network inferred

(C) Hierarchical clustering tree showing the Euclidean distance between the gene expression profiles of all the checkpoint kinase mutants. Clustering of the sample tree was bootstrapped (100 iterations); branch points with bootstrap values <100% are labeled.
(D) The refined model for the checkpoint-kinase-mediated transcriptional response indicates that the checkpoint-kinase-dependent transcriptional response to MMS treatment is primarily mediated by activation of Rad53 by Mec1 and Tel1 and that the Dun1-dependent transcriptional response represents a subset of the overall response. The blue circle indicates that the Dun1-dependent response is similar to Mec1-dependent response.
See also Table S2.

Please cite this article in press as: Jaehnig et al., Checkpoint Kinases Regulate a Global Network of Transcription Factors in Response to DNA Damage, Cell Reports (2013), http://dx.doi.org/10.1016/j.celrep.2013.05.041

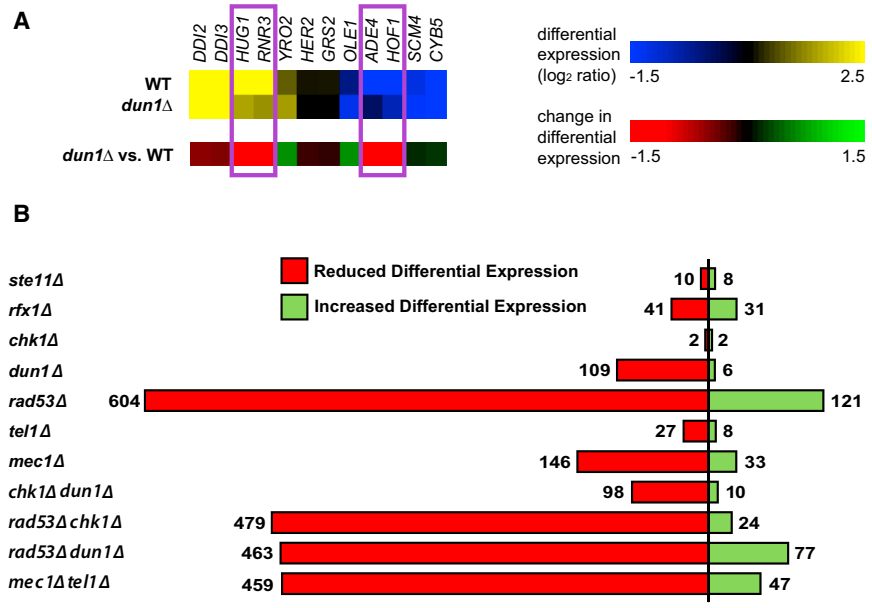

Figure 2. Identification of Genes Showing Checkpoint-Kinase-Dependent Differential Expression

(A) Example showing how deletion of *DUN1* affects DNA damage-induced changes in gene expression. The top panel shows gene expression of a selected set of genes from WT and the *dun1Δ* mutant strain, whereas the bottom panel (mutant versus WT) shows the effect of deleting the kinase on changes in gene expression.

(B) Bar graph of the total number of genes for which deleting the indicated kinase results in a statistically significant effect on DNA damage-induced differential expression. The relevant data are presented in Tables S2 and S3.

See also Tables S2, S3, S4, and S5.

for the set of Dun1-dependent genes. We found significant enrichment for targets of Rfx1 in both the Dun1- and Rfx1-dependent gene sets, confirming that Rfx1 regulates predicted Rfx1 targets and lies downstream of Dun1 (Figure 3B; Table S6). The combined network for TFs consistently inferred from all of the checkpoint kinase-dependent gene sets contained interactions between the checkpoint kinases and nine downstream TFs (Figures 3C, S1, and S2). Analysis of previously published expression data indicated that mutations in the nonessential TF genes (*MSN4*, *MBP1*, *SWI6*, *SWI4*, *GCN4*, *RFX1*, and *FKH2*) reduced expression of many MMS-induced genes whose expression was similarly affected by deletion of *RAD53* (Figures S3, S4, and S5) (Workman et al., 2006). In addition, the checkpoint kinases showed significant potential interactions with seven other TFs (Arg81, Cad1, Fkh1, Gln3, Hir2, Msn2, and Rph1), albeit with less consistency (Figure S1; Table S6).

GO enrichment analysis of the Rad53-dependent genes predicted to be targets of each TF in the Dun1-regulated branch of this network revealed that these TFs regulate genes involved in DNA metabolism (Rfx1), amino acid metabolism (Gcn4), cell division (Fkh2, Mcm1, and Ndd1), and rRNA processing (Fkh2 and Ndd1) (Figures 3C, S1, and S2; Table S7). These observations are consistent with previous studies implicating Rfx1 in nucleotide metabolism during the DDR (Huang et al., 1998), Gcn4 in stress responses induced by environmental amino acid imbalances (Hinnebusch and Fink, 1983; Yoon et al., 2004), and the complex containing Fkh2, Mcm1, and Ndd1 in promoting the G2 to M cell-cycle transition (Bähler, 2005). The network of TFs controlled by the checkpoint kinases (Figure 3C) did not include the Arg81, Rtg3, and Cad1 TFs shown in Figure 3B because enrichment of their targets was not consistently observed in the other checkpoint kinase mutants (Table S6). However, all the target genes that allowed us to infer connections for Dun1 with Arg81 and Rtg3 were also included in the set of Gcn4 targets (Figure 3B), suggesting that a limitation of this approach is that we cannot determine the specificity of TFs whose targets have a high degree of overlap. Finally, only 43% of the Dun1-dependent genes (47 out of 109) were included in this network (Figures 2C and 3B), indicating that Dun1 may also regulate other TFs that we could not identify using this approach.

The TFs acting downstream of Rad53, but not Dun1, included Msn4, which regulates responses to stress and temperature, and MBF (Swi6-Mbp1) and SBF (Swi6-Swi4), which regulates G1 to S transition in the cell cycle and expression of nucleic acid metabolism genes involved in DNA replication and repair (Figures 3C and S2; Table S7) (Sidorova and Breeden, 1993; Verma et al., 1992). At a lower threshold, enrichment for targets of Arg81, Rtg3, and Cad1 (also regulated by Dun1) and of Fkh1, Gln3, Hir2, and Msn4 and Rph1 (Dun1 independent) was also observed (Figure S1; Table S7). In summary, our analysis reveals a global transcriptional regulatory network in which Rad53 regulates at least Msn4 and the SBF/MBF complexes independently of Dun1 and Rfx1, Gcn4, and the Fkh2/Mcm1/Ndd1 complex via Dun1 (Figure 3C).

Rad53-Dependent Phosphorylation of TFs in the Checkpoint-Kinase-Mediated Response

To determine if the checkpoint kinase cascade regulates the TFs identified in this global network (Figure 3C) via phosphorylation, we used mass spectroscopy (MS) to compare the levels of phosphopeptides for each TF purified from a *rad53Δ* mutant with those same peptides purified from an isogenic WT strain (Figure 4; Table S8). (Rfx1 was not examined because its phosphoregulation by Rad53 and Dun1 has been described by Huang et al. (1998). Also note that Rph1, an additional TF included in Figure S1, has been shown to undergo Rad53-dependent, DNA damage-induced phosphorylation (Kim et al., 2002).) The *rad53Δ* mutant was the focus of this analysis because virtually the entire checkpoint-kinase-mediated transcriptional response to MMS was Rad53 dependent (Figures 1C and 3C). Because a single phosphosite was often seen in multiple peaks/peptides, we also calculated the total relative levels for all MS peaks

containing a given phosphosite to better determine the extent to which phosphorylation was affected by the *rad53Δ* mutation (Table 1).

We observed peptides with Rad53-dependent changes in phosphorylation from all eight TFs tested. In total, 34 phosphorylation sites (greater phosphorylation in WT) and 21 dephosphorylation sites (greater phosphorylation in the *rad53Δ* mutant) were observed in at least one of three independent experiments conducted for each TF (Figure 4). Ndd1, Msn4, Fkh2, Mbp1, and Swi6 had at least one site that showed a net reduction in phosphorylation in the *rad53Δ* mutant in at least two experiments (Table 1), whereas Gcn4, which may also be activated by the accumulation of unspliced mRNAs in response to DNA damage (Ghavidel et al., 2007), and Swi4 had sites showing a net reduction in phosphorylation in only one experiment. The only potential Rad53-dependent phosphorylation site on Mcm1 showed inconsistent results in different experiments (Table 1). Fkh2, Msn4, Ndd1, Mbp1, and Swi6 also had sites showing a net increase in phosphorylation in *rad53Δ* mutants in at least one experiment (Table 1), possibly due to activation of a phosphatase or inactivation of an intermediate kinase by Rad53. Fkh2, Mcm1, or Ndd1 activity may also be indirectly regulated by Hcm1, a transcriptional activator not included in the database we used to identify the TFs (Pramila et al., 2006). However, it is unlikely that Hcm1 plays a role in the regulation of these TFs because *HCM1* gene expression did not change in WT and was actually repressed by MMS treatment in *rad53Δ* mutants that failed to downregulate targets of Fkh2, Mcm1, and Ndd1 (Table S2). Interestingly, a single peptide on Swi6 contained six potential phosphorylation sites that could be separated into two groups. Peptides containing T169 and S170 showed Rad53-dependent phosphorylation, whereas peptides containing S176, S178, T179, and T182 (but not T169 or S170) were found either to not be changing or to show Rad53-dependent dephosphorylation when peptides with phosphorylation of multiple sites were observed (Figure 4; Table 1). Furthermore, we observed higher levels of peptides containing T169 or S170 in WT yeast treated with MMS compared to untreated yeast, whereas peptides containing only S176, S178, T179, and/or T182 were not induced by MMS (data not shown). MMS also induced phosphorylation of Rad53-dependent sites on Swi4 (S271) and Mbp1 (S133, S191, and S212).

Putative Rad53 consensus sites accounted for 17 of the 34 potential Rad53-dependent phosphorylation sites, including T169 and S170 on Swi6, S212 on Mbp1, and S271 on Swi4 (Table 1) (Sidorova and Breeden, 2003; Smolka et al., 2007). Meanwhile, only 2 of the 34 sites were Mec1/Tel1 consensus sites (Kim et al., 1999), only 2, which were also Rad53-dependent phosphorylation sites on Ndd1 and Mbp1, were Dun1 consensus sites, and only 1, which was also a Rad53-dependent site on Fkh2, was a Cdc28 consensus site (Sanchez et al., 1997; Songyang et al., 1994). Although the Dun1-dependent set of genes was enriched for targets of Gcn4, Fkh2, and Mcm1, we did not observe phosphorylation of Dun1 consensus phosphorylation sites on these TFs. These observations may reflect the fact that Rad53 and Dun1 consensus sites are not yet well defined. Regardless of whether phosphoregulation of these TFs occurs directly by Rad53 or Dun1 or indirectly by downstream kinases or phosphatases, it appears that nearly all of the TFs have Rad53-dependent phosphorylation sites that could contribute to transcriptional regulation.

Predicted G1 Targets of MBF Are Activated by MMS, whereas G2/M Targets of Fkh2/Mcm1/Ndd1 Are Repressed by Dun1 Independently of Cell-Cycle Arrest

Several of the TFs identified regulate cell-cycle progression (Bähler, 2005; Koch et al., 1993; Sidorova and Breeden, 1993; Verma et al., 1991). We, therefore, utilized the results of a previous analysis of cell-cycle-specific gene expression (Spellman et al., 1998) to investigate the relationship of the checkpoint-kinase-dependent transcriptional response to the cell cycle. As shown in Figure 5A and Table S9, the set of Rad53-dependent genes upregulated by MMS treatment was enriched for genes with peak expression in G1 phase, whereas the downregulated set was enriched for genes with peak expression in S, G2, and M phases. Specifically, G1-specific genes included upregulated genes predicted to be targets of Mbp1, Swi4, and Swi6, whereas G2/M phase genes included downregulated targets of Fkh2, Ndd1, and Mcm1 (Figure 5B; Table S9).

Previous studies have suggested two distinct models for how Rad53 regulates Swi6 during the DDR. Rad53 may inhibit expression of Swi6 target genes and, thus, cell-cycle progression (Sidorova and Breeden, 1997, 2003). Alternatively, Rad53 may activate the Mbp1/Swi6 (MBF) complex in response to DNA damage (Bastos de Oliveira et al., 2012; Travesa et al., 2012). In the network of putative Mbp1, Swi4, and Swi6 targets regulated by Rad53 (Figure 5C), the majority of Mbp1 target genes were upregulated during the MMS response. Taken together with the observation that the upregulated targets of Mbp1 and Swi6 were enriched for G1-specific genes (Figure 5B; Table S9), our results are consistent with the model in which Rad53 activates transcription by MBF in response to DNA damage. Furthermore, our GO enrichment analysis suggests that Rad53 most likely activates expression of MBF target genes involved in DNA replication and repair (Figures 3B and S2). However, just over half of the predicted targets (17 out of 31) of Swi4 and/or Swi6, but not Mbp1, were downregulated by MMS (Figure 5C), and downregulated targets of these TFs showed enrichment for G2/M genes (Figure 5B; Table S9). These results suggest that the Swi4/Swi6 (SBF) complex may play a different role in the transcriptional response to MMS treatment.

Of the remaining TFs in the checkpoint-kinase-dependent network (Figure 3C), only Fkh2, Mcm1, and Ndd1, which are also targets of Dun1, showed enrichment for cell-cycle-specific gene expression (Figure 5B; Table S9). Putative downregulated targets of all three of these TFs showed enrichment for G2/M genes, including *CDC5*, *CLB2*, *ACE2*, and *SWI5* (Figure 3B; Tables S4 and S9). Although deletion of *FKH2* affected expression of a small set of genes that was primarily upregulated by MMS (Figure S3), regulation of Mcm1 and Ndd1, the essential members of the complex, by the checkpoint kinases may be sufficient for mediating repression of G2/M targets.

Under the conditions used here, MMS causes a cell-cycle delay in S phase (the intra-S checkpoint; Figures 5D and S6) (Paulovich and Hartwell, 1995). This raises the question of whether repression of genes associated with the G2 to M

Please cite this article in press as: Jaehnig et al., Checkpoint Kinases Regulate a Global Network of Transcription Factors in Response to DNA Damage, Cell Reports (2013), http://dx.doi.org/10.1016/j.celrep.2013.05.041

Cell PRESS Open ACCESS

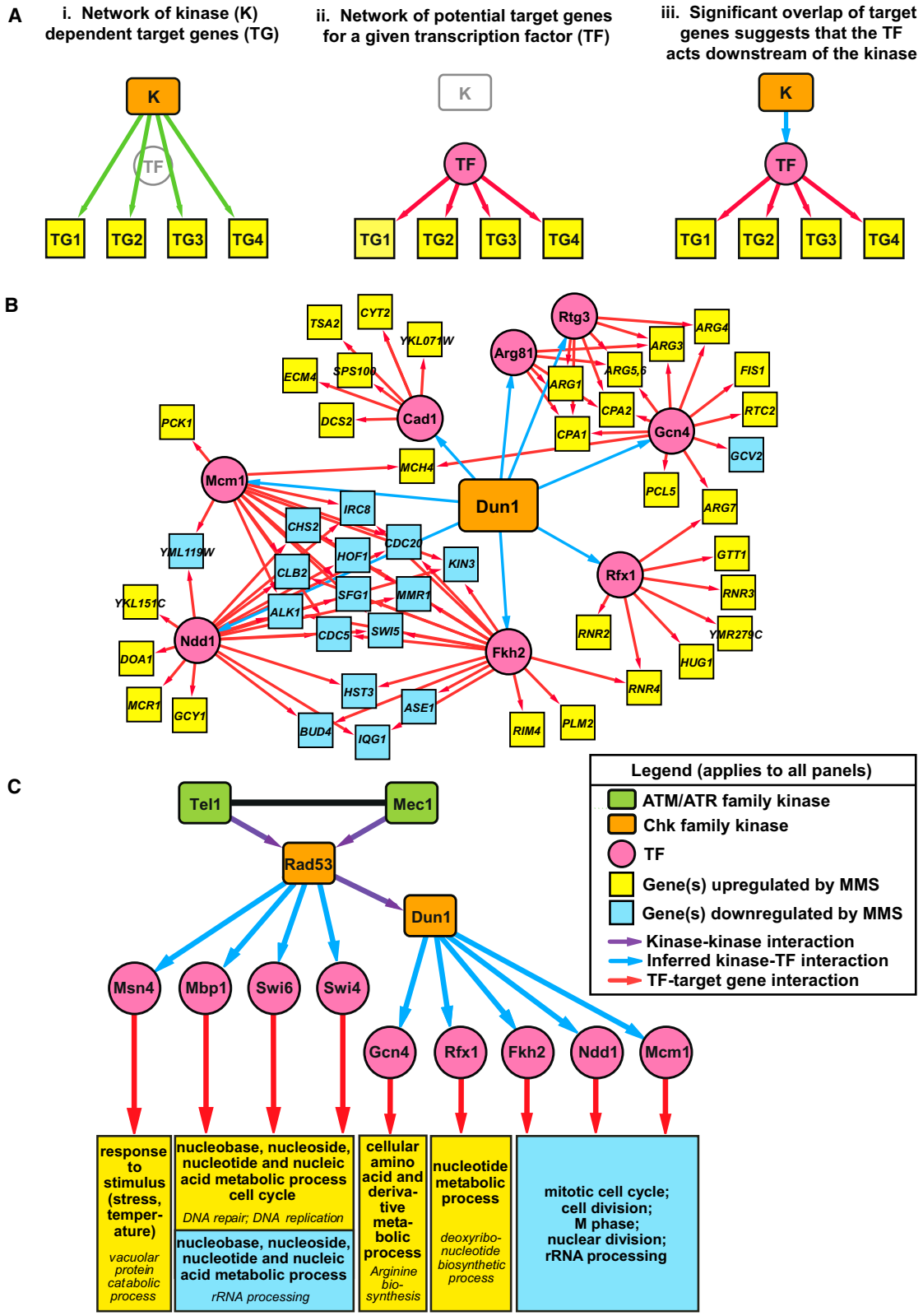

(legend on next page)

Cell PRESS
Open ACCESS

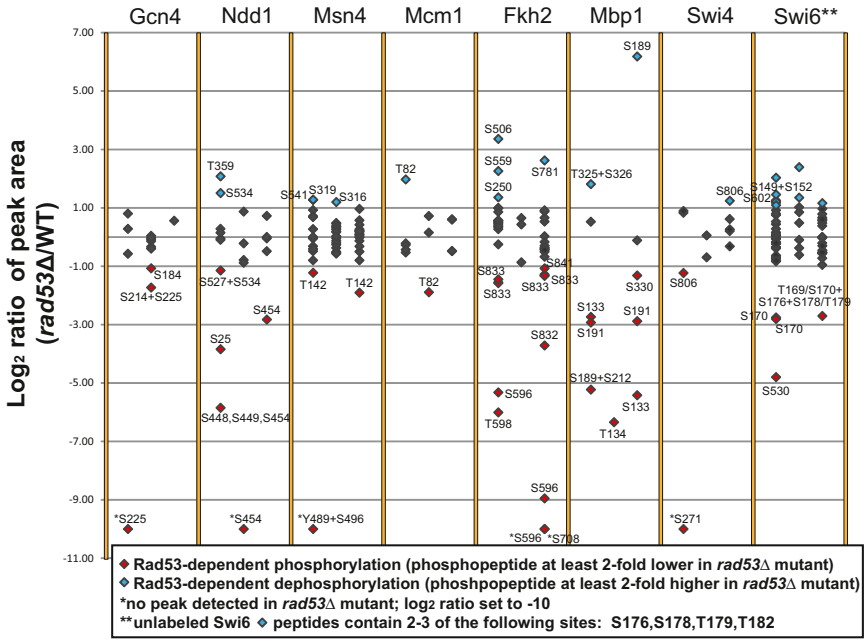

Figure 4. Rad53-Dependent Phosphorylation of Downstream TFs

The $\log_2$ ratios obtained from SILAC analysis of the *rad53Δ* mutant relative to WT for each individual peak identifying a peptide with a phosphorylation site are shown. Data for each of three independent experiments are shown as adjacent scatterplots for each TF. Complete data for all of the peptides identified are presented in Table S8.

phase transition was due to indirect effects associated with a greater proportion of cells residing in S phase during MMS treatment. As shown in Figure 5D, asynchronous populations of WT cells analyzed by fluorescence-activated cell sorting (FACS) were evenly distributed between cells with either 1 N or 2 N DNA content. However, MMS treatment resulted in a shift toward a greater population with 1 N DNA content and the appearance of a population of cells with S phase DNA content between 1 N and 2 N (Figure 5D). By contrast, the *rad53Δ* mutant strains were deficient in this checkpoint because MMS-treated *rad53Δ* mutant cells resembled untreated cells (Figures 5D and S6). Both the *mec1Δ* and *mec1Δtel1Δ* mutant strains also displayed this checkpoint defect, but the *dun1Δ* and *dun1Δchk1Δ* mutants had an intact intra-S checkpoint (Figures 5D and S6). Consistent with these results, release of α factor-arrested cells into MMS resulted in a delay in progression through S phase in both the *dun1Δ* mutant and WT, whereas the *rad53Δ* strain progressed rapidly through S phase (data not shown).

The observation that a *dun1Δ* deletion mutant arrests in S phase in response to MMS treatment (Figure 5D) even though deletion of *DUN1* prevented DNA damage-induced repression of predicted Fkh2, Mcm1, and Ndd1 targets with peak expression in G2/M (Figure S3) suggests that these genes are not repressed in WT cells as a result of DNA damage-induced cell-cycle arrest. Rather, Dun1 likely directly regulates DNA damage-induced repression of these genes by modulating the activity of the transcriptional complex consisting of Mcm1, Ndd1, and possibly Fkh2. Consistent with this, the expression profiles of *mec1Δ* and *dun1Δ* clustered together (Figure 1B), and the sets of Mec1- and Dun1-dependent genes overlapped by ~50% (Table S5) even though deletion of *MEC1* and *DUN1* resulted in a defect (no cell-cycle delay) and no defect in the intra-S checkpoint (cell-cycle delay) in response to MMS, respectively. However, the majority of Mcm1 and Ndd1 targets and approximately half of the predicted Fkh2 targets showed stronger defects in differential expression in the *rad53Δ* mutant than in the *dun1Δ* mutant (Figure S3). This may reflect a failure to arrest in response to MMS that leads to a higher proportion of cells expressing G2/M genes and/or an additional role for Rad53 in the direct regulation of these TFs. Consistent with the latter possibility, the most likely checkpoint-kinase-dependent phosphorylation sites on Fkh2 (S596) and Ndd1 (S454) were consensus sites for Rad53 (Table 1). In addition, most of the Rfx1 and Gcn4 targets showing differential expression in response to MMS treatment were affected more substantially

Figure 3. Implicating TFs as Downstream Effectors of the Checkpoint-Kinase-Dependent Transcriptional Response to DNA Damage

(A) Strategy used to identify kinase-TF interactions. (i) The kinase transcriptional regulatory network consists of interactions between the kinase and the set of target genes with kinase-dependent changes in gene expression. (ii) The TF regulatory network consists of predicted interactions between TFs and their target genes (Beyer et al., 2006). (iii) Significant overlap of target genes in the kinase and TF regulatory networks suggests that an interaction between the kinase and TF explains how the kinase regulates transcription of its target genes.

(B) The transcriptional regulatory network generated by applying this analysis to the Dun1-dependent set of target genes.

(C) A global transcriptional regulatory network showing kinase-TF interactions mediating the checkpoint-kinase-dependent transcriptional response to DNA damage. Kinase-TF interactions were only included in this network if four of the seven checkpoint-kinase-dependent gene sets showed enrichment for targets of the TF (see Table S6 for enrichment analysis and Figure S1 for a larger network that includes TFs enriched in two or more kinase-dependent gene sets). For simplicity, the target genes were replaced with modules showing the enriched GO terms in the sets of Rad53-dependent genes predicted to be targets of the TF (selected from Table S7). Fkh2, Ndd1, and Mcm1 form a transcriptional complex, and Swi6 forms distinct transcriptional complexes with Mbp1 (MBF) and Swi4 (SBF). Therefore, the Fhh2/Ndd1/Mcm1 and MBF/SBF target genes are represented in overlapping modules of enriched GO terms (see Figure S2). Fkh1 was omitted because nearly all of its predicted targets comprise a subset of the target genes of the Fkh2/Ndd1/Mcm1 complex. GO terms in italics are subcategories of the main GO terms listed above.

See also Tables S6 and S7 and Figures S1 and S2.

Please cite this article in press as: Jaehnig et al., Checkpoint Kinases Regulate a Global Network of Transcription Factors in Response to DNA Damage, Cell Reports (2013), http://dx.doi.org/10.1016/j.celrep.2013.05.041

Cell PRESS
Open ACCESS

Table 1. Analysis of Rad53-Dependent Phosphorylation Sites Identified in Figure 4A

TF	Phosphosite[a]	Kinase Consensus Recognition Sequences[b]	*rad53*Δ/WT[c] Run 1	Run 2	Run 3
Gcn4	**S184**	Chk1; Rad53-A,C	ND	0.48	ND
Gcn4	**S214**	Rad53-A	1.21	0.84	ND
Gcn4	**S225**		0.00	0.78	ND
Gcn4	**S214+S225**		ND	0.30	ND
Msn4	**T142**	Rad53-B	0.43	ND	0.27
Msn4	*S316*	Rad53-C	0.75	1.79	1.05
Msn4	*S319*		1.47	0.79	1.63
Msn4	**Y489**		0.56	1.24	0.71
Msn4	**S496**	Rad53-C	0.00	ND	ND
Msn4	*S541*		2.41	ND	ND
Msn4	**Y489+S496**		0.00	ND	ND
Fkh2	*S250*		2.56	ND	ND
Fkh2	*S506*	Mec1/Tel1	10.27	ND	ND
Fkh2	*S559*		1.81	ND	0.81
Fkh2	**S596**	Rad53-A,B	0.03	ND	0.00
Fkh2	**T598**		0.02	ND	ND
Fkh2	**S708**	Rad53-C	1.38	ND	0.67
Fkh2	**S714**		ND	ND	0.41
Fkh2	*S781*		ND	ND	6.16
Fkh2	**S832**	Rad53-B	1.37	1.57	1.61
Fkh2	**S833**	Rad53-C; Cdc28	0.59	1.36	0.43
Fkh2	**S841**		ND	ND	0.48
Mcm1	T82	Rad53-A; Mec1/Tel1	3.93	0.27	1.51
Ndd1	**S25**		0.07	ND	ND
Ndd1	*T359*	Rad53-C	4.22	ND	ND
Ndd1	**S448**		0.02	ND	ND
Ndd1	**S449**	Rad53-B	0.02	ND	ND
Ndd1	**S454**	Rad53-A	0.02	0.00	0.14
Ndd1	**S527**	Rad53-A,C; Chk1; Dun1	1.20	0.58	1.03
Ndd1	S534		1.94	ND	ND
Ndd1	**S527+S534**		0.45	ND	ND
Mbp1	**S133**		0.15	ND	0.02
Mbp1	**T134**		ND	0.01	ND
Mbp1	S189	Mec1/Tel1	0.03	ND	72.72
Mbp1	**S191**	Chk1; Dun1	0.13	ND	0.14
Mbp1	**S212**	Rad53-A,B,C	0.03	ND	ND
Mbp1	**S330**	Rad53-B,C	ND	ND	0.40
Mbp1	*T325*		3.51	ND	ND
Mbp1	*S326*	Rad53-C	3.51	ND	ND
Mbp1	**S189+S212**		0.03	ND	ND
Mbp1	*T325+S326*		3.51	ND	ND
Swi4	**S271**	Rad53-A	0.00	ND	ND
Swi4	S806		0.43	1.04	2.36
Swi6	*S149*	Rad53-A	0.99	ND	0.52
Swi6	*S152*	Rad53-B	1.12	ND	0.52
Swi6	**T169**	Rad53-B,C	1.74	ND	0.15
Swi6	**S170**	Rad53-A,C	0.37	0.59	0.15
Swi6	*S176*		0.94	1.23	1.09
Swi6	*S178*		1.27	1.43	1.02
Swi6	*T179*		1.07	1.34	1.19
Swi6	*T182*		1.75	1.97	1.55
Swi6	**S530**		0.04	ND	ND
Swi6	*S602*		2.13	ND	ND
Swi6	*S149+S152*		1.62	ND	0.52
Swi6	*S176+T179*		1.32	1.58	1.24
Swi6	**T169+S176+T179**		ND	ND	0.15
Swi6	**S170+S176+S178**		0.79	0.65	0.15
Swi6	*S176+S178+T179*		2.74	2.31	1.65
Swi6	*S176+S178+T182*		ND	2.43	2.03
Swi6	*S176+T179+T182*		1.37	2.55	1.70
Swi6	*S178+T179+T182*		4.09	5.25	2.16

ND, phosphosite not detected or not quantifiable.

[a]Phosphorylation sites identified in Figure 4 as potentially phosphorylated (bold) or dephosphorylated (italics) in a Rad53-dependent manner or both (normal).

[b]Potential consensus sites for Rad53 are denoted as Rad53-A for the consensus sequence reported by Smolka et al. (2007), whereas sites characterized by Sidorova and Breeden are classified as either complete (Rad53-B,C) or as one-half sites as follows: Rad53-B is the one-half site amino terminal to the phosphosite, and Rad53-C is the one-half site carboxy-terminal to the phosphosite (Sidorova and Breeden, 2003). Consensus recognition sequences reported previously for Mec1/Tel1, Dun1, Chk2, and Cdc28 were used for this analysis (Hutchins et al., 2000; Kim et al., 1999; Sanchez et al., 1997; Songyang et al., 1994).

[c]For each experiment run, the total area of all the MS1 peaks corresponding to peptides with the phosphosite in the *rad53*Δ mutant was divided by the total area of the equivalent MS1 peaks in the WT strain and normalized to the median ratio for all peptides observed in the experiment.

by deletion of *RAD53* than by deletion of *DUN1* even though did they not show cell-cycle-specific gene expression (Figure S4). Finally, deleting *TEL1* in a *mec1Δ* mutant resulted in reduced DNA damage-induced regulation of many additional genes even though the *mec1Δ* mutation was sufficient to cause a complete defect in MMS-induced cell-cycle delay (Figures 2B and 5D). These observations suggest that the broad role that Rad53 plays in regulating transcription in response to MMS is not solely a consequence of cell-cycle arrest.

A Network of TFs Mediates Gene Expression Independently of the Checkpoint Kinases

Although nearly 1,700 genes were differentially expressed in response to MMS, only ~600 of these showed significantly reduced differential expression in the *rad53Δ* mutant,

suggesting a substantial transcriptional response that is checkpoint kinase independent. Therefore, we evaluated the set of differentially expressed genes that was not checkpoint kinase dependent for enrichment of putative TF targets. The differentially expressed genes were divided into a checkpoint-kinase-dependent set of 547 genes (224 genes with expression disrupted in only one of the nine kinase mutants were excluded) and a checkpoint-kinase-independent set of 901 genes, and enrichment for TF targets was computed for each set (Figure 6A; Table S10). We observed enrichment for predicted targets of 18 TFs in the checkpoint-kinase-dependent set and enrichment for targets of 10 different TFs (Cad1, Hsf1, Hap1, Hap4, Rcs1, Rds1, Rpn4, Yap1, and Yap7; Sut1 was of borderline significance) in the checkpoint-kinase-independent set (Figure 6A). Targets of Cad1 (Yap2) were also overrepresented among the Dun1-dependent genes (Figure 3B), but nearly all of the checkpoint-kinase-independent targets of Cad1 were also targets of Yap1 and Yap7 (Figure S7). Thus, there is a strong possibility that Yap1 and/or Yap7 mediates expression of these targets and that Cad1 was implicated in the checkpoint-kinase-independent response to MMS simply because it shares predicted target genes. Similarly, most of the predicted targets of Rds1 were also targets of either Hap1 or Yap1 and Yap7 (Figure S7). Although many predicted targets of Hap1 were also predicted targets of Hap4, and whereas Yap1 and Yap7 share several common predicted targets, unique predicted targets of each of these TFs were also checkpoint kinase independent (Figure S7). In total, 294 of the 901 checkpoint-kinase-independent genes were predicted targets of Cad1, Hsf1, Hap1, Hap4, Rcs1, Rds1, Rpn4, Sut1, Yap1, or Yap7.

To confirm the role of these TFs in the checkpoint-kinase-independent transcriptional response, we analyzed previously published expression profiles of *rpn4Δ* and *yap1Δ* mutants (Workman et al., 2006) and performed expression profiling of five other TFs (Hap1, Hap4, Rcs1, Sut1, and Yap7; Cad1 and Rds1 were not included because their predicted targets are likely regulated by other TFs, and Hsf1 was not included because it is essential) and found that these TFs all regulated checkpoint-kinase-independent genes (Figures 6B, S8, S9, and S10). Interestingly, all of these TFs were also found to regulate checkpoint-kinase-dependent genes (Figure 6B) even though the Beyer et al. (2006) analysis only predicted that 16 of the 264 kinase-dependent genes affected by deletion of the TFs were targets of the corresponding TFs.

GO enrichment analysis indicated that these TFs regulate stress response genes. Analysis of both predicted TF target genes in the checkpoint-kinase-independent DDR network (Figure S7) and of TF-dependent gene sets (Figure 6B) indicated that Rcs1 and Yap1 activate and Hap1 represses genes involved in the oxidative stress response (Table S7). Analysis of predicted TF targets in the checkpoint-kinase-independent network also suggested that Hsf1 activates temperature response genes, Rpn4 activates genes regulating proteolysis, and Hap4 represses nucleotide metabolism genes (Figure S7). Given that differential expression of these genes was observed in both cells arrested at the intra-S checkpoint (WT and *dun1Δ* mutant, Figure 5D) and in cells that were checkpoint defective (*rad53Δ* and *mec1Δ* mutants, Figure 5D), it is unlikely that differential expression of these genes was a consequence of a shift in the proportion of cells from one stage of the cell cycle to another in response to MMS treatment.

DISCUSSION

Here, we integrated data generated using genomic and proteomic approaches to characterize the function of the checkpoint kinases in the transcriptional response induced by DNA damage. Our studies documented a number of key results.

(1) Tel1 was dispensable for the transcriptional response elicited by MMS, whereas simultaneous deletion of both *MEC1* and *TEL1* had a far greater effect than deletion of *MEC1* alone even though deletion of *MEC1* causes a complete defect in the cell-cycle delay induced by MMS.
(2) Deletion of *RAD53* affected the MMS-induced transcriptional response to the same extent as codeletion of *MEC1* and *TEL1.*
(3) Rad53 and Mec1/Tel1 similarly mediated differential expression of ~500 genes, of which ~100 and ~150 were also regulated by Dun1 and Mec1, respectively. These checkpoint-kinase-dependent genes included targets of a set of nine TFs, at least five of which were phosphorylated in a Rad53-dependent fashion.
(4) A distinct group of at least seven TFs regulates differential gene expression in response to MMS independently of the checkpoint kinase cascade.
(5) The transcriptional response does not appear to be the indirect consequence of perturbation of the cell cycle by MMS.

These results indicate that the MMS-induced transcriptional response involves a considerably more complex network than previously appreciated.

Previous studies have shown that overexpression of *TEL1* can suppress and deletion of *TEL1* can modestly enhance the DNA damage sensitivity of a *mec1Δ* mutant, suggesting that Mec1 and Tel1 have similar activities (Morrow et al., 1995). However, the checkpoint response to MMS, as assessed by MMS-induced S phase delay and inhibition of nuclear division, is entirely dependent on Mec1 (Paulovich and Hartwell, 1995). Furthermore, MMS-induced phosphorylation of Rad53 is almost entirely dependent on Mec1; only a very low level of residual MMS-induced phosphorylation of Rad53 was seen in a *mec1* mutant, and this phosphorylation appeared to be Tel1 dependent (Sanchez et al., 1996). In the gene expression analysis reported here, deletion of *TEL1* had little effect on MMS-induced gene expression, whereas the *mec1Δtel1Δ* double mutant affected differential expression to a much greater extent than the *mec1Δ* single mutant. Mec1 and Tel1 primarily appeared to activate Rad53 because the *rad53Δ* mutants had differential gene expression profiles that were similar to that of the *mec1Δtel1Δ* double mutant. Deletion of *CHK1* did not affect MMS-induced gene expression, consistent with observations that Chk1 is primarily involved in the G2/M checkpoint, whereas MMS, under the conditions used here, primarily activates the intra-S

Please cite this article in press as: Jaehnig et al., Checkpoint Kinases Regulate a Global Network of Transcription Factors in Response to DNA Damage, Cell Reports (2013), http://dx.doi.org/10.1016/j.celrep.2013.05.041

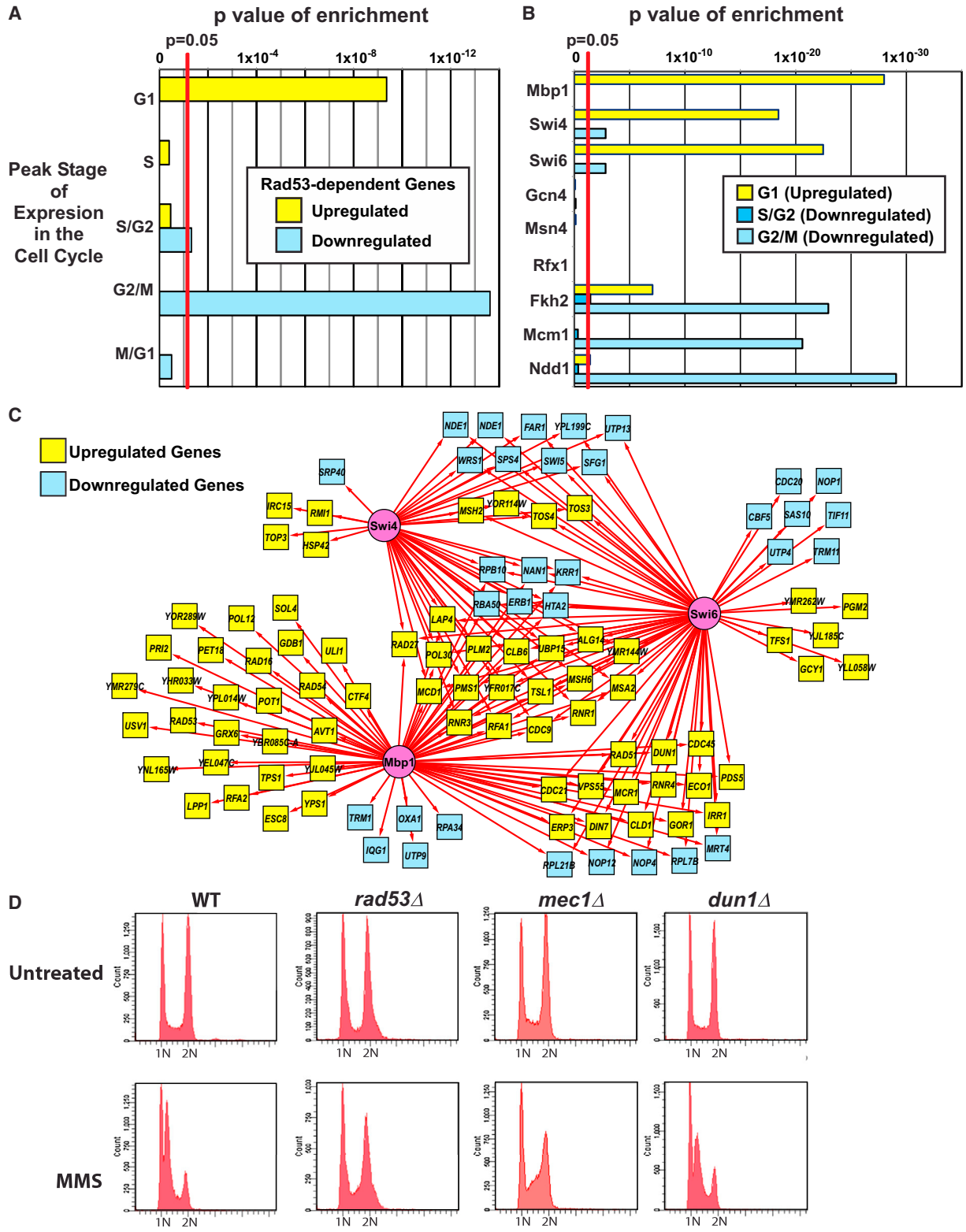

Figure 5. Investigating the Relationship of the Checkpoint-Kinase-Dependent Transcriptional Response with the Cell Cycle

(A) Checkpoint-kinase-dependent genes with peak expression in G1 phase are upregulated in response to MMS treatment, whereas genes with peak expression in S, G2, and M phases are downregulated. Graph shows p values for enrichment of genes reported to have peak expression at different stages of the cell cycle (Spellman et al., 1998) among the upregulated and downregulated sets of Rad53-dependent genes.

(legend continued on next page)

checkpoint (Liu et al., 2000; Paulovich and Hartwell, 1995; Sanchez et al., 1999). Interestingly, deletion of *DUN1*, which acts downstream of Rad53 (Allen et al., 1994; Bashkirov et al., 2003), did not affect differential expression of targets of TFs in the Dun1 branch of the transcriptional response to the same extent that the *rad53Δ* mutation did (Figures S3, S4, and S5). This suggests that Rad53 also acts on Rfx1, Fkh2, Mcm1, Ndd1, and Gcn4 in a Dun1-independent manner. In contrast, Rad53 appears to regulate expression of targets of Msn4, Swi6, Swi4, and Mbp1 through Dun1-independent mechanisms, consistent with previous results showing that SBF (Swi4/Swi6) and MBF (Mbp1/Swi6) are directly regulated by Rad53 (Bastos de Oliveira et al., 2012; Sidorova and Breeden, 1997, 2003; Travesa et al., 2012). Overall, our results show that the MMS-induced checkpoint-kinase-dependent transcriptional response is primarily mediated by activation of Rad53 by Mec1 and Tel1 leading to the activation of downstream Dun1-dependent and Dun1-independent branches. This transcriptional response is far more dependent on Tel1 than MMS-induced cell-cycle delay or Rad53 phosphorylation is. The simplest explanation for these results is that the low level of residual Rad53 phosphorylation seen in *mec1Δ* mutants is sufficient to at least partially regulate transcriptional but not other checkpoint responses. As such, this study provides a more comprehensive network of the checkpoint-kinase-mediated transcriptional response than the Mec1-mediated response previously reported by Gasch et al. (2001).

The observation that deletion of *MEC1* or *DUN1* had similar effects on differential gene expression in response to MMS treatment is consistent with previous results by Gasch et al. (2001). One possible explanation for this observation is that activation of Dun1 by Rad53 is solely Mec1 dependent (Tel1 cannot compensate for the loss of Mec1). Possible explanations for this would be that activation of Dun1 by Rad53 might require a scaffold containing Mec1 or that the interaction between Rad53 and Dun1 might require phosphorylation of at least one of these proteins by Mec1 specifically. Dun1 does contain a consensus site (S176) for Mec1/Tel1 that is phosphorylated in vivo and can serve as a substrate for Mec1 phosphorylation in vitro (Albuquerque et al., 2008; Mallory et al., 2003). Mutation of this site and the two other Mec1/Tel1 consensus sites on Dun1 did not cause the increased MMS sensitivity caused by deletion of *DUN1*; however, Mec1 and Tel1 were still able to phosphorylate this mutant to a lesser extent in vitro, suggesting the existence of additional Mec1/Tel1 phosphorylation sites (Mallory et al., 2003). These observations suggest that activation of Dun1 is more complex than a linear Mec1 > Rad53 > Dun1 pathway.

The fact that most of the TFs predicted to act downstream of Rad53 were phosphorylated in a Rad53-dependent manner suggests that they are regulated by phosphorylation. Although much of this regulation may be due to phosphorylation by Rad53, phosphorylation by Dun1 is also Rad53 dependent (Allen et al., 1994). Thus, the phosphorylation sites identified on TFs in the Dun1-dependent transcriptional response are likely regulated by Dun1. Another possibility is that other kinases or phosphatases downstream of Rad53 and Dun1 may be responsible for phosphorylation of the TFs. In fact, a number of Rad53-dependent sites observed did not fit Rad53 or Dun1 consensus phosphorylation sites or Mec1/Tel1 consensus phosphorylation sites (Table 1). We also observed Rad53-dependent dephosphorylation at sites on several TFs, presumably mediated by activation of downstream phosphatases or inhibition of downstream kinases, suggesting alternative mechanisms for indirect phosphoregulation of TFs by Rad53. Although beyond the scope of this study, the effects of mutating these phosphorylation sites on MMS-induced transcriptional profiles in future experiments will better delineate the mechanisms by which the checkpoint kinases regulate TFs.

Nearly 900 genes were differentially expressed in response to MMS independently of the checkpoint kinase cascade, and ~300 of these checkpoint-kinase-independent genes were predicted to be targets of a distinct network of TFs (Hsf1, Hap1, Hap4, Rcs1, Rpn4, Sut1, Yap1, and Yap7). Direct analysis of the nonessential TFs in this network confirmed that they regulate expression of checkpoint-kinase-independent genes but also revealed that they regulate checkpoint-kinase-dependent genes (Figures 6B, S8, S9, and S10). Most of the kinase-dependent genes showing reduced differential expression in these TF mutants were not predicted targets of the corresponding TFs in the Beyer et al. analysis (Beyer et al., 2006). Because this analysis incorporated ChIP-Chip and predicted TF recognition site data to assign direct TF target predictions, the simplest explanation for this finding is that these checkpoint-kinase-dependent genes are regulated indirectly by these TFs.

A previous study identified genes that showed Mec1- and Dun1-independent regulation in response to MMS but likely misclassified many checkpoint-kinase-dependent genes as checkpoint-kinase-independent because, unlike our study, *rad53Δ* and *mec1Δ tel1Δ* mutants were not analyzed (Gasch et al., 2001). Although we have not ruled out the possibility that there could be some checkpoint-independent genes that are regulated redundantly by the Chk kinases (Rad53, Dun1, and Chk1) and, thus, only revealed by analyzing a *rad53Δ dun1Δ chk1Δ* triple mutant, these kinases should all be downstream of Mec1 and Tel1. That study also mentioned that a small number of Mec1- and Dun1-independent genes were shown to be targets of Yap1, Hsf1, and Hap1 in other studies. In contrast, our enrichment analysis provides a more rigorous systematic approach for identifying specific TFs downstream of both the checkpoint-kinase-dependent and -independent damage responses and has implicated many more TFs in the DDR than previously

(B) Applying the same enrichment analysis for cell-cycle-specific expression to Rad53-dependent genes that are predicted targets of the TFs shown in Figure 3C reveals that upregulated targets of Mbp1, Swi4, Swi6, Fkh2, and Ndd1 are enriched for G1 genes, downregulated targets of Fkh2 are enriched for S/G2 genes, and downregulated targets of Swi4, Swi6, Fkh2, Mcm1, and Ndd1 are enriched for G2/M genes (Table S9).

(C) The Rad53-dependent transcriptional regulatory network for predicted targets of Mbp1, Swi4, and Swi6.

(D) FACS analysis of asynchronous cultures of untreated and MMS-treated WT, *rad53Δ*, *mec1Δ*, and *dun1Δ* strains (see Figure S6 for other strains).

See also Tables S4 and S9 and Figure S6.

Please cite this article in press as: Jaehnig et al., Checkpoint Kinases Regulate a Global Network of Transcription Factors in Response to DNA Damage, Cell Reports (2013), http://dx.doi.org/10.1016/j.celrep.2013.05.041

Cell PRESS
Open ACCESS

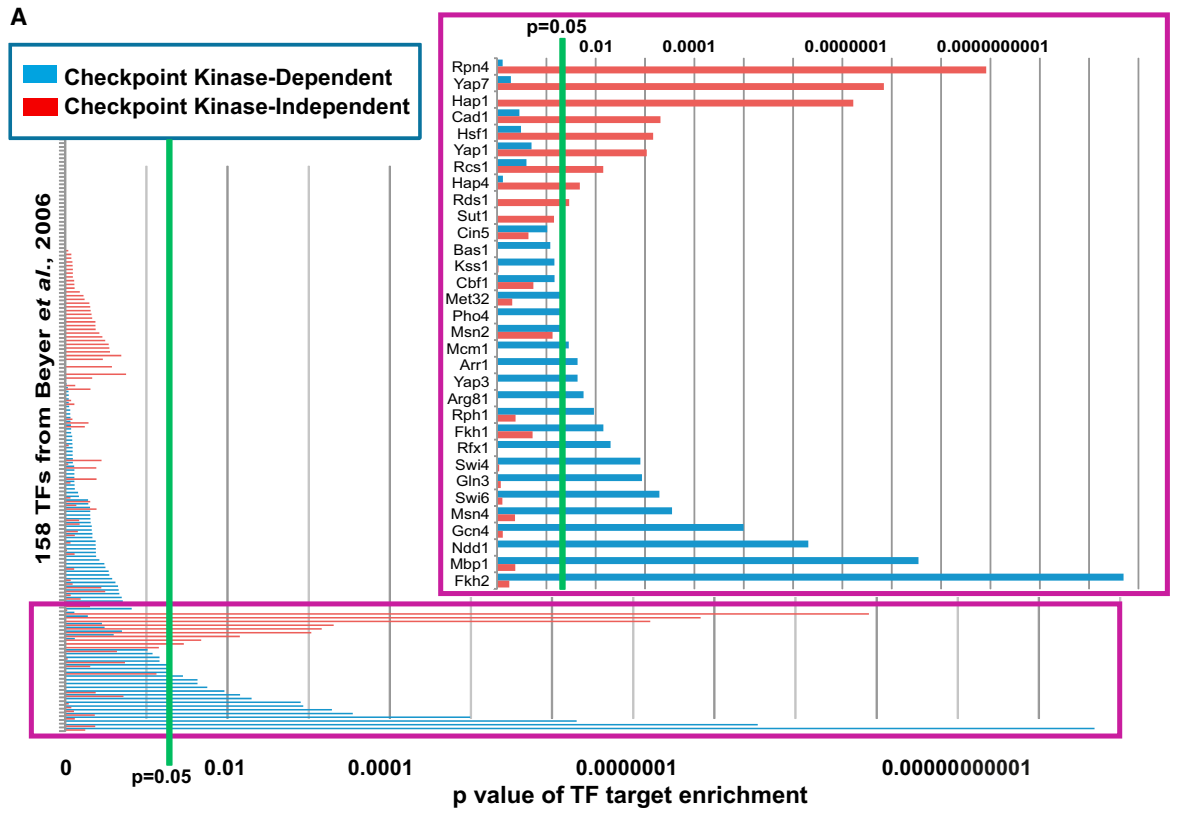

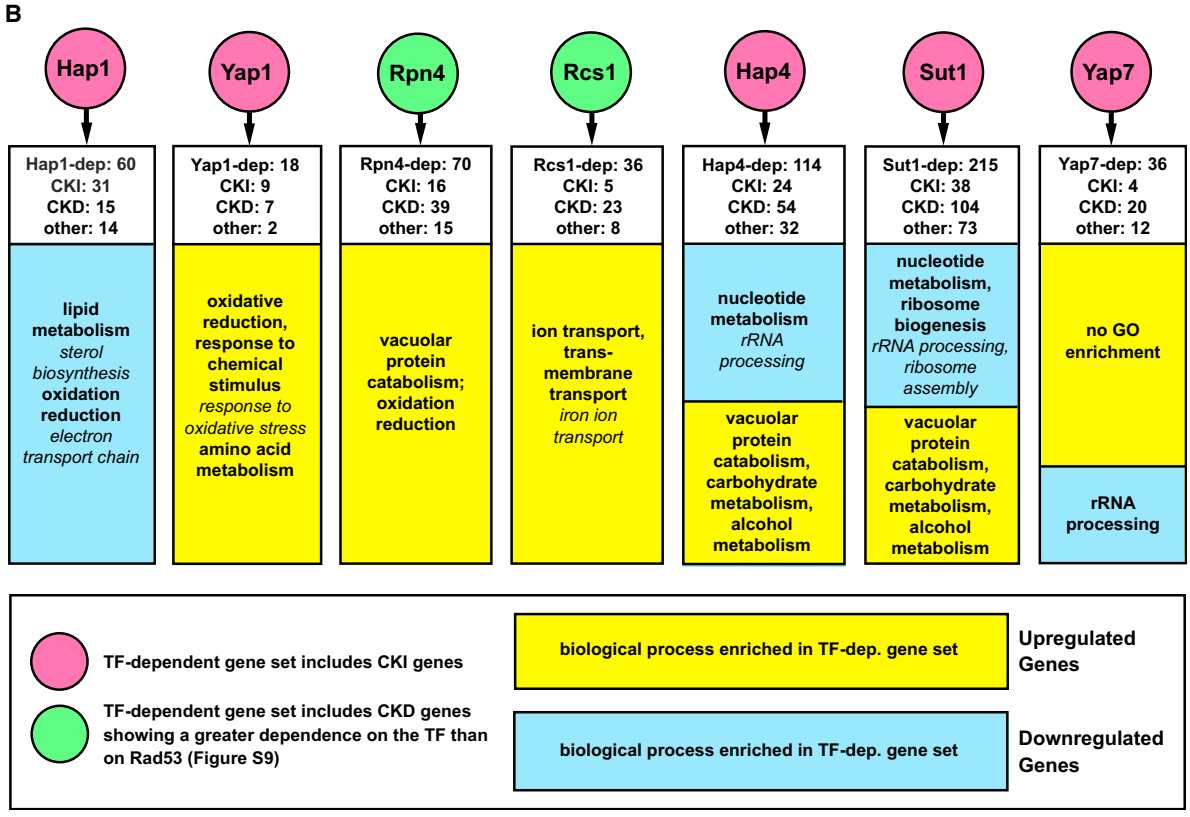

(legend on next page)

appreciated. Specifically, we found that Hsf1, Rcs1, and Yap1 targets involved in stress responses were primarily upregulated in response to MMS, whereas targets of Hap1 and Hap4 involved in oxidation reduction were primarily downregulated. Gasch et al. also observed that known Yap1 and Hap1 targets were differentially expressed in response to MMS but not ionizing radiation and that potential Hsf1 targets were upregulated by MMS but downregulated by ionizing radiation and suggested that the MMS-induced, Mec1-independent transcriptional response was not specific for DNA damage but rather was a consequence of cellular oxidative stress induced by MMS treatment (Gasch et al., 2001). Given our observation that the checkpoint-kinase-dependent transcriptional response also involves TFs that participate in stress responses (Msn4 and Gcn4, Figure 3C), it seems probable that MMS induces gene expression changes associated with general stress responses in parallel with those associated with the DDR. Future studies using a diversity of DNA-damaging agents and involving direct analysis of individual TFs should more precisely define the components of the kinase-independent gene expression network that are DNA damage induced and those that are nonspecific stress responses.

EXPERIMENTAL PROCEDURES

S. cerevisiae Strains

The strains used in the expression-profiling experiments were Mat-a strains derived either from the *S. cerevisiae* knockout collection or from BY4741 (YSC1053; Open Biosystems, Thermo Scientific) using standard gene knockout methods. WT (*sml1Δ*) and *rad53Δsml1Δ* versions of arginine plus lysine auxotrophic strains containing TAP-tagged TFs were used for the SILAC experiments. All strains are listed in Table S1.

Gene Expression Profiling

The gene expression experiments were carried out as described previously (Workman et al., 2006) using Agilent microarrays (Yeast v.2). Two independent experiments comparing MMS-treated (0.03%) with untreated cells were performed on two independent isolates for each strain.

Processing and Analysis of Expression Array Data

The median intensities of technically replicated probes were analyzed with the *Li*near *M*odels of *M*icroarray data package (LIMMA) (Smyth, 2005). LIMMA was also employed to compare and detect significant differences in differential expression between the kinase or TF deletion and WT strains for each gene. Data are included in Table S2 and summarized in Table S3.

Enrichment Analysis

The sets of genes that were categorized as kinase dependent (i.e., genes with significantly reduced differential expression in each mutant; Figure 3C; Table S6), as genes that were kinase dependent in at least two of the experiments (the checkpoint-kinase-dependent set; Figure 6A; Table S10), or as genes that were not kinase dependent in any experiment (the checkpoint-kinase-independent set; Figure 6A; Table S10) were evaluated for enrichment of targets of each TF (Beyer et al., 2006) using the hypergeometric test. Enrichment analysis for cell-cycle-regulated genes (Figures 5A and 5B; Table S9) was executed by evaluating the sets of Rad53-dependent up- and downregulated genes (both all Rad53-dependent genes and genes that are targets of a given TF) were instead evaluated for enrichment with genes having peak expression at the specified cell-cycle stages (Spellman et al., 1998).

FACS

Asynchronous cultures were grown using the same conditions used for the microarray experiment. For synchronized cell-cycle experiments, cultures were arrested in G1 with 5 μg/ml α factor (AnaSpec), washed, and incubated in YPD containing 20 μg/ml nocodazole and 100 μg/ml pronase E (Sigma-Aldrich) with or without 0.03% MMS. Cells were stained with 1 μM SYTOX Green (Invitrogen) and analyzed by FACS.

Identification of Rad53-Dependent Phosphorylation Sites by SILAC

Cultures of WT and *rad53Δ* strains with TAP-tagged TFs were grown in synthetic media supplemented with amino acids including either normal "light" L-arginine and L-lysine or deuterium-labeled "heavy" L-arginine and L-lysine (L-Arginine-$^{13}C_6$,$^{15}N_4$ hydrochloride [608033] and L-Lysine-$^{13}C_6$,$^{15}N_2$ hydrochloride [608041] from Sigma-Aldrich) as described previously by Chen et al. (2010). After treatment with 0.03% MMS for 1 hr, equal amounts of both cultures were combined, the TAP-tagged TF was purified, digested with trypsin, enriched for phosphopeptides by IMAC (Stensballe and Jensen, 2004), and analyzed by MS-MS. The data for peaks identified as peptides from each TF are shown in Table S8. See Extended Experimental Procedures for detailed Experimental Procedures.

ACCESSION NUMBERS

The GEO accession number for the microarray data reported in this paper is GSE40351.

SUPPLEMENTAL INFORMATION

Supplemental Information includes Extended Experimental Procedures, ten figures, and ten tables and can be found with this article online at http://dx.doi.org/10.1016/j.celrep.2013.05.041.

ACKNOWLEDGMENTS

The authors would like to thank R.D.K. and T.G.I. lab members for helpful discussions and the Huilin Zhou lab for help with the mass spectrometry experiments. This work was supported by NIH grants F32 GM086899 (to E.J.J.), ES014811 (to T.G.I.), GM26017 (to R.D.K.), and GM085764 (to T.G.I.).

Received: August 28, 2012
Revised: April 4, 2013
Accepted: May 24, 2013
Published: June 27, 2013

Figure 6. Identification of TFs Mediating Checkpoint-Kinase-Independent Gene Expression in Response to MMS Treatment

(A) The set of genes that was checkpoint kinase dependent (i.e., showed reduced differential expression in at least two of the checkpoint kinase mutants) and the set of genes that was checkpoint-kinase- independent (i.e., not affected by any of the checkpoint kinase mutations) show enrichment for targets of distinct sets of TFs. Enrichment for TF targets was performed as in Figure 3, and the p values for enrichment for targets of all 158 TFs are shown here and in Table S10. The inset shows TFs with enrichment p values that are <0.1.

(B) Expression profiling confirms that the predicted TFs regulate checkpoint-kinase-independent (CKI) gene expression and identifies checkpoint-kinase-dependent (CKD) genes regulated by the TFs (see Table S2 and Figures S8–S10 for expression profile data). TF-dependent genes for Hap1, Hap4, Rcs1, Sut1, and Yap7 were identified by expression profiling of TF mutants as in Figure 2 (see Table S3), whereas deletion-buffered genes from Workman et al. (2006) were analyzed for Rpn4 and Yap1. White boxes indicate the number of CKD and CKI genes that showed reduced differential expression in the TF mutant. GO terms in italics are subcategories of the main GO terms listed.

See also Tables S2, S3, S4, S7, and S10 and Figure S7.

REFERENCES

Albuquerque, C.P., Smolka, M.B., Payne, S.H., Bafna, V., Eng, J., and Zhou, H. (2008). A multidimensional chromatography technology for in-depth phosphoproteome analysis. Mol. Cell. Proteomics *7*, 1389–1396.

Allen, J.B., Zhou, Z., Siede, W., Friedberg, E.C., and Elledge, S.J. (1994). The SAD1/RAD53 protein kinase controls multiple checkpoints and DNA damage-induced transcription in yeast. Genes Dev. *8*, 2401–2415.

Bähler, J. (2005). Cell-cycle control of gene expression in budding and fission yeast. Annu. Rev. Genet. *39*, 69–94.

Bardwell, L. (2004). A walk-through of the yeast mating pheromone response pathway. Peptides *25*, 1465–1476.

Bashkirov, V.I., Bashkirova, E.V., Haghnazari, E., and Heyer, W.D. (2003). Direct kinase-to-kinase signaling mediated by the FHA phosphoprotein recognition domain of the Dun1 DNA damage checkpoint kinase. Mol. Cell. Biol. *23*, 1441–1452.

Basrai, M.A., Velculescu, V.E., Kinzler, K.W., and Hieter, P. (1999). NORF5/HUG1 is a component of the MEC1-mediated checkpoint response to DNA damage and replication arrest in *Saccharomyces cerevisiae*. Mol. Cell. Biol. *19*, 7041–7049.

Bastos de Oliveira, F.M., Harris, M.R., Brazauskas, P., de Bruin, R.A., and Smolka, M.B. (2012). Linking DNA replication checkpoint to MBF cell-cycle transcription reveals a distinct class of G1/S genes. EMBO J. *31*, 1798–1810.

Beyer, A., Workman, C., Hollunder, J., Radke, D., Möller, U., Wilhelm, T., and Ideker, T. (2006). Integrated assessment and prediction of transcription factor binding. PLoS Comput. Biol. *2*, e70.

Branzei, D., and Foiani, M. (2006). The Rad53 signal transduction pathway: replication fork stabilization, DNA repair, and adaptation. Exp. Cell Res. *312*, 2654–2659.

Branzei, D., and Foiani, M. (2009). The checkpoint response to replication stress. DNA Repair (Amst.) *8*, 1038–1046.

Chen, S.H., Albuquerque, C.P., Liang, J., Suhandynata, R.T., and Zhou, H. (2010). A proteome-wide analysis of kinase-substrate network in the DNA damage response. J. Biol. Chem. *285*, 12803–12812.

Gasch, A.P., Huang, M., Metzner, S., Botstein, D., Elledge, S.J., and Brown, P.O. (2001). Genomic expression responses to DNA-damaging agents and the regulatory role of the yeast ATR homolog Mec1p. Mol. Biol. Cell *12*, 2987–3003.

Ghavidel, A., Kislinger, T., Pogoutse, O., Sopko, R., Jurisica, I., and Emili, A. (2007). Impaired tRNA nuclear export links DNA damage and cell-cycle checkpoint. Cell *131*, 915–926.

Hinnebusch, A.G., and Fink, G.R. (1983). Positive regulation in the general amino acid control of *Saccharomyces cerevisiae*. Proc. Natl. Acad. Sci. USA *80*, 5374–5378.

Huang, M., Zhou, Z., and Elledge, S.J. (1998). The DNA replication and damage checkpoint pathways induce transcription by inhibition of the Crt1 repressor. Cell *94*, 595–605.

Hutchins, J.R., Hughes, M., and Clarke, P.R. (2000). Substrate specificity determinants of the checkpoint protein kinase Chk1. FEBS Lett. *466*, 91–95.

Ideker, T., Thorsson, V., Ranish, J.A., Christmas, R., Buhler, J., Eng, J.K., Bumgarner, R., Goodlett, D.R., Aebersold, R., and Hood, L. (2001). Integrated genomic and proteomic analyses of a systematically perturbed metabolic network. Science *292*, 929–934.

Kim, S.T., Lim, D.S., Canman, C.E., and Kastan, M.B. (1999). Substrate specificities and identification of putative substrates of ATM kinase family members. J. Biol. Chem. *274*, 37538–37543.

Kim, E.M., Jang, Y.K., and Park, S.D. (2002). Phosphorylation of Rph1, a damage-responsive repressor of PHR1 in *Saccharomyces cerevisiae*, is dependent upon Rad53 kinase. Nucleic Acids Res. *30*, 643–648.

Koch, C., Moll, T., Neuberg, M., Ahorn, H., and Nasmyth, K. (1993). A role for the transcription factors Mbp1 and Swi4 in progression from G1 to S phase. Science *261*, 1551–1557.

Kolodner, R.D., Putnam, C.D., and Myung, K. (2002). Maintenance of genome stability in *Saccharomyces cerevisiae*. Science *297*, 552–557.

Liu, Y., Vidanes, G., Lin, Y.C., Mori, S., and Siede, W. (2000). Characterization of a *Saccharomyces cerevisiae* homologue of *Schizosaccharomyces pombe* Chk1 involved in DNA-damage-induced M-phase arrest. Mol. Gen. Genet. *262*, 1132–1146.

Mallory, J.C., Bashkirov, V.I., Trujillo, K.M., Solinger, J.A., Dominska, M., Sung, P., Heyer, W.D., and Petes, T.D. (2003). Amino acid changes in Xrs2p, Dun1p, and Rfa2p that remove the preferred targets of the ATM family of protein kinases do not affect DNA repair or telomere length in *Saccharomyces cerevisiae*. DNA Repair (Amst.) *2*, 1041–1064.

Morrow, D.M., Tagle, D.A., Shiloh, Y., Collins, F.S., and Hieter, P. (1995). TEL1, an *S. cerevisiae* homolog of the human gene mutated in ataxia telangiectasia, is functionally related to the yeast checkpoint gene MEC1. Cell *82*, 831–840.

Paulovich, A.G., and Hartwell, L.H. (1995). A checkpoint regulates the rate of progression through S phase in *S. cerevisiae* in response to DNA damage. Cell *82*, 841–847.

Pramila, T., Wu, W., Miles, S., Noble, W.S., and Breeden, L.L. (2006). The Forkhead transcription factor Hcm1 regulates chromosome segregation genes and fills the S-phase gap in the transcriptional circuitry of the cell cycle. Genes Dev. *20*, 2266–2278.

Putnam, C.D., Jaehnig, E.J., and Kolodner, R.D. (2009). Perspectives on the DNA damage and replication checkpoint responses in *Saccharomyces cerevisiae*. DNA Repair (Amst.) *8*, 974–982.

Rouse, J., and Jackson, S.P. (2002). Interfaces between the detection, signaling, and repair of DNA damage. Science *297*, 547–551.

Sanchez, Y., Desany, B.A., Jones, W.J., Liu, Q., Wang, B., and Elledge, S.J. (1996). Regulation of RAD53 by the ATM-like kinases MEC1 and TEL1 in yeast cell cycle checkpoint pathways. Science *271*, 357–360.

Sanchez, Y., Zhou, Z., Huang, M., Kemp, B.E., and Elledge, S.J. (1997). Analysis of budding yeast kinases controlled by DNA damage. Methods Enzymol. *283*, 398–410.

Sanchez, Y., Bachant, J., Wang, H., Hu, F., Liu, D., Tetzlaff, M., and Elledge, S.J. (1999). Control of the DNA damage checkpoint by chk1 and rad53 protein kinases through distinct mechanisms. Science *286*, 1166–1171.

Sidorova, J., and Breeden, L. (1993). Analysis of the SWI4/SWI6 protein complex, which directs G1/S-specific transcription in *Saccharomyces cerevisiae*. Mol. Cell. Biol. *13*, 1069–1077.

Sidorova, J.M., and Breeden, L.L. (1997). Rad53-dependent phosphorylation of Swi6 and down-regulation of CLN1 and CLN2 transcription occur in response to DNA damage in *Saccharomyces cerevisiae*. Genes Dev. *11*, 3032–3045.

Sidorova, J.M., and Breeden, L.L. (2003). Rad53 checkpoint kinase phosphorylation site preference identified in the Swi6 protein of *Saccharomyces cerevisiae*. Mol. Cell. Biol. *23*, 3405–3416.

Smolka, M.B., Albuquerque, C.P., Chen, S.H., and Zhou, H. (2007). Proteome-wide identification of in vivo targets of DNA damage checkpoint kinases. Proc. Natl. Acad. Sci. USA *104*, 10364–10369.

Smyth, G.K. (2005). Limma: linear models for microarray data. In Bioinformatics and Computational Biology Solutions using R and Bioconductor, R.V.C. Gentleman, S. Dudoit, R. Irizarry, and W. Huber, eds. (New York: Springer), pp. 397–420.

Songyang, Z., Blechner, S., Hoagland, N., Hoekstra, M.F., Piwnica-Worms, H., and Cantley, L.C. (1994). Use of an oriented peptide library to determine the optimal substrates of protein kinases. Curr. Biol. *4*, 973–982.

Spellman, P.T., Sherlock, G., Zhang, M.Q., Iyer, V.R., Anders, K., Eisen, M.B., Brown, P.O., Botstein, D., and Futcher, B. (1998). Comprehensive identification of cell cycle-regulated genes of the yeast *Saccharomyces cerevisiae* by microarray hybridization. Mol. Biol. Cell *9*, 3273–3297.

Stensballe, A., and Jensen, O.N. (2004). Phosphoric acid enhances the performance of Fe(III) affinity chromatography and matrix-assisted laser desorption/ionization tandem mass spectrometry for recovery, detection and sequencing of phosphopeptides. Rapid Commun. Mass Spectrom. *18*, 1721–1730.

Travesa, A., Kuo, D., de Bruin, R.A., Kalashnikova, T.I., Guaderrama, M., Thai, K., Aslanian, A., Smolka, M.B., Yates, J.R., 3rd, Ideker, T., and Wittenberg, C. (2012). DNA replication stress differentially regulates G1/S genes via Rad53-dependent inactivation of Nrm1. EMBO J. *31*, 1811–1822.

Van Driessche, N., Demsar, J., Booth, E.O., Hill, P., Juvan, P., Zupan, B., Kuspa, A., and Shaulsky, G. (2005). Epistasis analysis with global transcriptional phenotypes. Nat. Genet. *37*, 471–477.

Verma, R., Patapoutian, A., Gordon, C.B., and Campbell, J.L. (1991). Identification and purification of a factor that binds to the Mlu I cell cycle box of yeast DNA replication genes. Proc. Natl. Acad. Sci. USA *88*, 7155–7159.

Verma, R., Smiley, J., Andrews, B., and Campbell, J.L. (1992). Regulation of the yeast DNA replication genes through the Mlu I cell cycle box is dependent on SWI6. Proc. Natl. Acad. Sci. USA *89*, 9479–9483.

Workman, C.T., Mak, H.C., McCuine, S., Tagne, J.B., Agarwal, M., Ozier, O., Begley, T.J., Samson, L.D., and Ideker, T. (2006). A systems approach to mapping DNA damage response pathways. Science *312*, 1054–1059.

Yoon, S., Govind, C.K., Qiu, H., Kim, S.J., Dong, J., and Hinnebusch, A.G. (2004). Recruitment of the ArgR/Mcm1p repressor is stimulated by the activator Gcn4p: a self-checking activation mechanism. Proc. Natl. Acad. Sci. USA *101*, 11713–11718.

Cell PRESS
Open ACCESS

EXTENDED EXPERIMENTAL PROCEDURES

Saccharomyces cerevisiae *Strains*

The strains used in the expression profiling experiments were derived either from the *S. cerevisiae* knockout collection or from BY4741, the parental mat-a strain used to generate the collection (YSC1053, Open Biosystems, Thermo Scientific) using standard gene knockout methods. All mutations were verified by PCR amplification using primers designed to amplify each specific insertion. Two independent strain isolates were used in each experiment. The wild-type background for the transcription factor mutants (except *rfx1Δ*) was BY4741, while the wild-type background for the checkpoint kinase mutants and control strains (including *rfx1Δ*) was BY4741 with *SML1* deleted. Two of the *ste11Δ* experiments were performed in the BY4741 background, while the remaining two experiments were performed in the *sml1Δ* background. Since deletion of *SML1* did not affect gene expression (Figure 1C; Table S3), the two sets of *ste11Δ* experiments were combined for the analysis presented here. Wild-type (*sml1Δ*) and *rad53Δsml1Δ* versions of an arginine and lysine auxotrophic strain were used for the SILAC experiments. These strains were then used to construct strains in which each transcription factor was fused with a modified version of the TAP tag at the C terminus of the native TF gene locus linked to the KAN^R marker (the TAF tag) (Chen et al., 2007). Each TAP-tagged strain was verified by analysis of PCR products generated using a primer internal to the tagged TF and a primer in the TAP tag as well as by Western blotting of cell lysates using an antibody recognizing the TAP tag (1:2000 peroxidase anti-peroxidase, Sigma). The genotypes for all strains constructed for this study are shown in Table S1.

Gene Expression Profiling

The gene expression experiments were carried out as described previously (Workman et al., 2006). For these experiments, 100 ml cultures for each strain were grown to an OD_{600} density of 0.8-1.0 at 30°C in a shaker set to 200 rpm, split into two 50 ml cultures, and incubated for one additional hour either in the presence (MMS-treated) or absence (untreated) of 0.03% MMS (methyl methanesulfonate; Sigma 129925). Cells were then harvested by centrifugation, frozen in liquid nitrogen, and stored at −80°C. RNA was isolated from the frozen cells by hot acid phenol extraction and ethanol precipitation, and an Ambion Poly(A)Purist kit (AM1916) was used to isolate mRNA from these RNA samples. The Superscript Direct cDNA Labeling System (Invitrogen, L1015-03) was then used for reverse transcription on 2 μg of mRNA to generate cDNA that was labeled with either Cy3-dUTP or Cy5-dUTP (GE Healthcare, PA53022 and PA55022 respectively), and cDNA was purified from these reactions using an illustra CyScribe GFX Purification kit (GE Healthcare, 27-9606-01). 20 pmol of both the Cy3 labeled and the Cy5 labeled samples were hybridized to each array, following the Two-Color Microarray-Based Gene Expression Analysis protocol provided by Agilent. Slides were scanned at a resolution of 5 μm with an Agilent microarray scanner. Two independent experiments were performed on two independent isolates for each strain. cDNA from treated and untreated samples were labeled with Cy3 or Cy5 with the dyes reversed in biological replicates for each isolate to correct for dye bias effects. In total, four independent experiments were performed for each strain.

Processing and Analysis of Expression Array Data

GenePix 6.0 (Molecular Devices) was used for feature extraction to obtain median Cy3 and Cy5 intensities for each probe in the array. The median intensities of technically replicated probes were analyzed by the LInear Models of Microarray data package (LIMMA) (Smyth, 2005). Data was LOESS and quantile normalized and subsequently fitted to a linear model to assess the significance of differential expression in each strain for every gene in the genome. MultiExperiment Viewer (MeV) 4.5 was used to cluster the LRs for each experiment by Euclidean distance using the HCL Support Tree algorithm with 100 iterations of bootstrapping to generate the sample tree. PHYLIP version 3.69 was used to generate an unrooted hierarchical tree from the Newick dendrogram obtained from the clustering analysis (Figure 1C). LIMMA was also employed to compare and detect significant differences in differential expression between the kinase deletion and wild-type strains for each gene. For this comparison, the LIMMA package provided us with a LR for each gene that represented the difference between the mutant and the wild-type LRs [$LR_{KOvsWT} \approx (LR_{KO[MMS/untreated]} - LR_{WT[MMS/untreated]})$]. Thus, the LR_{KOvsWT} value is positive in the case where the gene is downregulated in wild-type ($LR_{WT[MMS/untreated]} < 0$) but no longer changing in the kinase mutant ($LR_{KO[MMS/untreated]} \approx 0$) and negative in the case where the gene is upregulated in wild-type ($LR_{WT[MMS/untreated]} > 0$) but no longer changing in the kinase mutant ($LR_{KO[MMS/untreated]} \approx 0$). However, both of these cases represent situations where differential expression, whether it be upregulated or downregulated expression, was reduced by deletion of the kinase. Thus, we modified the LR_{KOvsWT} value to reflect the change in the magnitude of differential expression rather than the direct difference between the mutant and wild-type LRs in order to obtain a $\Delta DE[LR_{KOvsWT}]$ value that is negative when differential expression is reduced and positive when differential expression is increased in the kinase mutant. LIMMA analysis of the checkpoint kinase mutant strains and the transcription factor mutant strains was performed separately; the same array data was used for both sets of analyses for the following strains: BY4741, *sml1Δ*, *ste11Δ*, *rfx1Δ*, *dun1Δ*, and *rad53Δ*. Log ratios (base 2) and differential expression calls for each gene for each comparison analyzed are included in Table S2 and summarized in Table S3. The wild-type strain for the transcription factor mutant analysis was BY4741 while the wild-type strains for the checkpoint kinase mutant analysis were RDKY7796 and 7797, which are *sml1Δ* derivatives of BY4741.

Enrichment Analysis

The sets of genes that were categorized as kinase-dependent for each kinase (i.e., genes with significantly decreased differential expression in the mutant compared to wild-type; Figure 3C; Table S6) and as genes that were kinase-dependent in at least two of the experiments (the checkpoint kinase-dependent gene set; Figure 6A; Table S10) or as genes that were not kinase-dependent in any experiment (the checkpoint kinase-independent gene set; Figure 6A; Table S10) were evaluated for enrichment of targets of each TF from Beyer et al. (Beyer et al., 2006). Specifically, the Hypergeometric test was used to determine if the set of genes that were both kinase-dependent and predicted TF targets was significantly greater than expected by chance given the proportion of the genome represented by each parent set. This statistical test was executed for each TF for each experiment. The set of p-values generated from this analysis was then subjected to multiple test hypothesis correction with Benjamini-Hochberg (BH) procedure (Hochberg and Benjamini, 1990). Enrichment analysis for cell cycle regulated genes (Figures 5A and 5B; Table S9) was executed using the same procedure, but the sets of Rad53-dependent up- and downregulated genes (both all Rad53-dependent genes and genes that are targets of a given TF) were instead evaluated for enrichment with genes having peak expression at the specified cell cycle stages in the Spellman et al. study (Spellman et al., 1998). The BINGO Cytoscape plugin (version 2.44) was used to analyze GO term enrichment (Maere et al., 2005).

Fluorescence-Activated Cell Sorting

Asynchronous cell cultures were grown using the same conditions as described above for the microarray experiment, but on a smaller scale (3 ml untreated and MMS-treated cultures). The synchronized cell cycle experiments were conducted as described previously (Enserink et al., 2009). Briefly, overnight cultures were washed with deionized water, diluted to an OD_{600} of 0.3, and arrested in G1 by incubation for 3 hr in the presence of 5 μg/ml alpha-factor (AnaSpec, Inc.). Cells were then split into two equal cultures, washed two times with YPD, and resuspended in YPD containing 20 μg/ml Nocodazole and 100 μg/ml Pronase E (Sigma). Both 0.03% MMS treated and untreated cultures were incubated with shaking at 30°C. Samples were collected every 15 min for 1 hr and at 100 min after the addition of MMS. About 0.5-1.0 $x10^7$ cells from each sample were washed and permeabilized with cold 70% EtOH. Cells were then resuspended in 50mM Na-Citrate buffer pH 7.0, sonicated (5 pulses 1 s each), and incubated overnight at 37°C in 50 mM Na-Citrate buffer supplemented with 0.25 mg/ml RNase A (USB Corporation) and 1 mg/ml Proteinase K (Sigma). Finally, cells were stained in the dark for 1 hr with 1 μM SYTOX Green (Invitrogen) and analyzed using a B&D LSRII FACS instrument.

Identification of Rad53-Dependent Phosphorylation Sites by SILAC

Both wild-type and *rad53Δ* strains for each TAP-tagged TF were grown to an OD_{600} of 0.8-1.0 at 30°C in a shaker at 200 rpm in separate 2 L cultures containing synthetic media supplemented with amino acids as described previously (Chen et al., 2010). To distinguish between proteins from the two samples, one culture was supplemented with normal "light" L-arginine and L-lysine, while the other was supplemented with "heavy" L-arginine and L-lysine (labeled with deuterium; L-Arginine-$^{13}C_6$,$^{15}N_4$ hydrochloride (608033) and L-Lysine-$^{13}C_6$,$^{15}N_2$ hydrochloride (608041) from Aldrich). After treatment with 0.03% MMS for one hour, equal amounts (as determined by OD_{600} measurements) of both cultures were mixed together and washed two times with deionized water, and the harvested cells were frozen in liquid nitrogen. Lysates were prepared from each cell pool and the TAP-tagged transcription factor was purified using the first step of the TAP tag purification protocol (Rigaut et al., 1999). Briefly, this involved lysing the pellets in 80-100 ml of NP40 lysis buffer with 5 one min bursts (with three min rests between each burst) in a bead beater (Biospec), followed by centrifugation for 1 hr at 15,500 rpm in a Sorvall SA-600 rotor using an RC5C centrifuge, binding protein from the supernatant to 600 μl of IgG Sepharose 6 Fast Flow resin (GE Healthcare, 52-2083-00 AH) at 4°C for 4-6 hr., washing two times with IPP150 buffer, and eluting with 3 ml SDS elution buffer after a 5 min incubation at room temperature. The NP40 lysis buffer consisted of 25 mM Tris pH 8.0, 150 mM NaCl, 0.1% NP40, 6 mM Na2HPO4, 4 mM NaH2PO4, 2 mM EDTA, 50 mM NaF, 1 mM DTT, 1x Protease Inhibitor cocktail set IV (Calbiochem, 539136), and 1x Phosphatase Inhibitor cocktail set II (Calbiochem, 524625). The IPP150 wash buffer contained 10 mM Tris pH 8.0 and 150 mM NaCl, and the SDS elution buffer consisted of 1% SDS in 50 mM Tris pH 8.0. Protein was precipitated from the eluate by incubating with 3 volumes of 1:1 acetone:ethanol on ice for at least one hr and harvested by centrifugation at 14,500 rpm for 15 min at 4°C. The protein pellet was then resuspended in 200 μl of 6 M urea. The samples were reduced by incubating with 10 mM DTT for 40 min at 42°C and alkylated by incubation with 50 mM iodoacetamide for 30 min at room temperature. Alkylation was halted by adding an additional 10 mM DTT and incubating for 1 min at room temperature. After diluting to 1M urea, the samples were then digested with 1-3 μg Trypsin (Promega, V5111) overnight at 37°C. Tryptic peptides were purified from the digests using 100 mg C18 Sep-Pak columns (Waters, WAT023590). 1%–5% of the eluate was dehydrated in a Savant Speed-Vac Plus (SC110A), resuspended in 0.1% trifluoroacetic acid, and analyzed by mass spectroscopy (MS). Immobilized Metal Affinity Chromatography was (IMAC) used to enrich for phosphopeptides from the remainder of each tryptic digest (Stensballe and Jensen, 2004). After dehydrating the IMAC eluates using a Speedvac, the peptides were resuspended in 0.1% TFA and 25%–75% of the resulting phosphopeptide mixture was subjected to nano-liquid C18 chromatography followed by MS-MS on a ThermoFinnegan LTQ Orbitrap. The TransProteomic Pipeline was used to analyze the MS data. Sorcerer (Sequest) was used for the initial identification of the peptides from the MS2 scans. Xpress analysis of the Sequest data allowed us to determine the areas of the MS1 peaks for the identified peptides and the peaks corresponding to the same peptides in the other sample. The use of "light" and "heavy" arginine and lysine in the two samples allowed direct comparison of the same phosphopeptide (area of the MS1 peak) from both samples in the same mass

spectroscopy experiment. All of the peptides identified, along with areas and intensities of the corresponding peaks and ratios of the peak areas in the *rad53Δ* sample relative to the wild-type sample are reported in Table S8.

SUPPLEMENTAL REFERENCES

Chen, S.H., Smolka, M.B., and Zhou, H. (2007). Mechanism of Dun1 activation by Rad53 phosphorylation in *Saccharomyces cerevisiae*. J. Biol. Chem. *282*, 986–995.

Enserink, J.M., Hombauer, H., Huang, M.E., and Kolodner, R.D. (2009). Cdc28/Cdk1 positively and negatively affects genome stability in *S. cerevisiae*. J. Cell Biol. *185*, 423–437.

Gasch, A.P., Spellman, P.T., Kao, C.M., Carmel-Harel, O., Eisen, M.B., Storz, G., Botstein, D., and Brown, P.O. (2000). Genomic expression programs in the response of yeast cells to environmental changes. Mol. Biol. Cell *11*, 4241–4257.

Hochberg, Y., and Benjamini, Y. (1990). More powerful procedures for multiple significance testing. Stat. Med. *9*, 811–818.

Maere, S., Heymans, K., and Kuiper, M. (2005). BiNGO: a Cytoscape plugin to assess overrepresentation of gene ontology categories in biological networks. Bioinformatics *21*, 3448–3449.

Rigaut, G., Shevchenko, A., Rutz, B., Wilm, M., Mann, M., and Séraphin, B. (1999). A generic protein purification method for protein complex characterization and proteome exploration. Nat. Biotechnol. *17*, 1030–1032.

Tishkoff, D.X., Filosi, N., Gaida, G.M., and Kolodner, R.D. (1997). A novel mutation avoidance mechanism dependent on *S. cerevisiae* RAD27 is distinct from DNA mismatch repair. Cell *88*, 253–263.

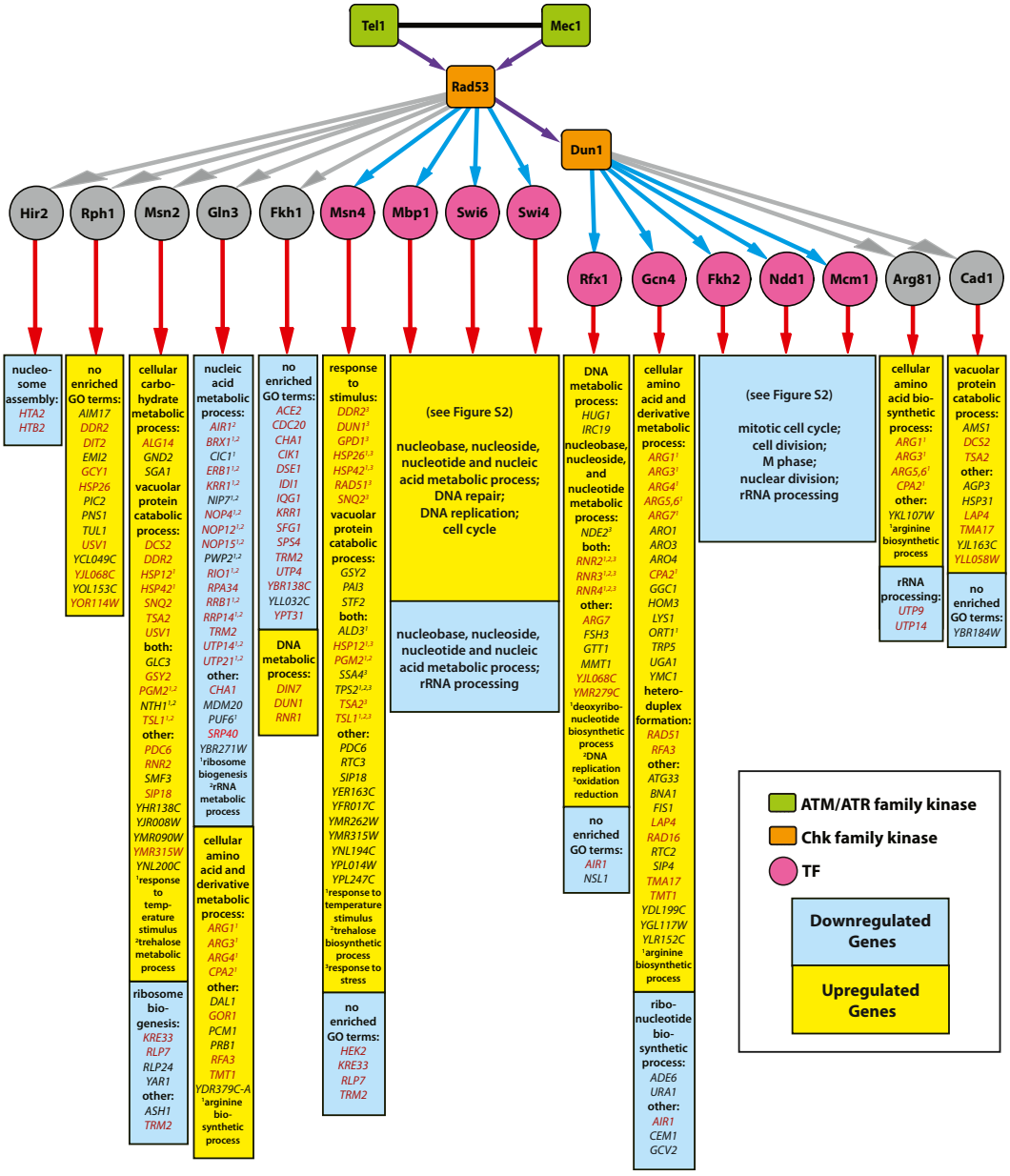

Figure S1. Network Diagram Indicating the Checkpoint-Kinase-Regulated TFs, Predicted Downstream Target Genes, and Selected GO Terms for Those Targets, Excluding Targets of Complexes Containing Swi4, Swi6, or Mbp1 and Fkh2, Ndd1, or Mcm1, Related to Figure 3

All Rad53-dependent genes predicted to be targets of each TF that showed significant enrichment in at least two of the checkpoint kinase-dependent gene sets (Table S6) are included and are grouped by associated GO terms from Table S7. TFs in purple are those shown in Figure 3C while TFs in gray are additional TFs implicated by only 2-3 of the checkpoint kinase-dependent gene sets. Also included in gray is Fkh1, which was not included in Figure 3C because nearly all of its predicted targets are contained within a subset of the targets of the Fkh2/Mcm1/Ndd1 complex (Figure S2) and are more likely regulated by that complex. Genes in black are unique targets of the indicated TF, while genes in red are also targets of other TFs. See also Figure S2.

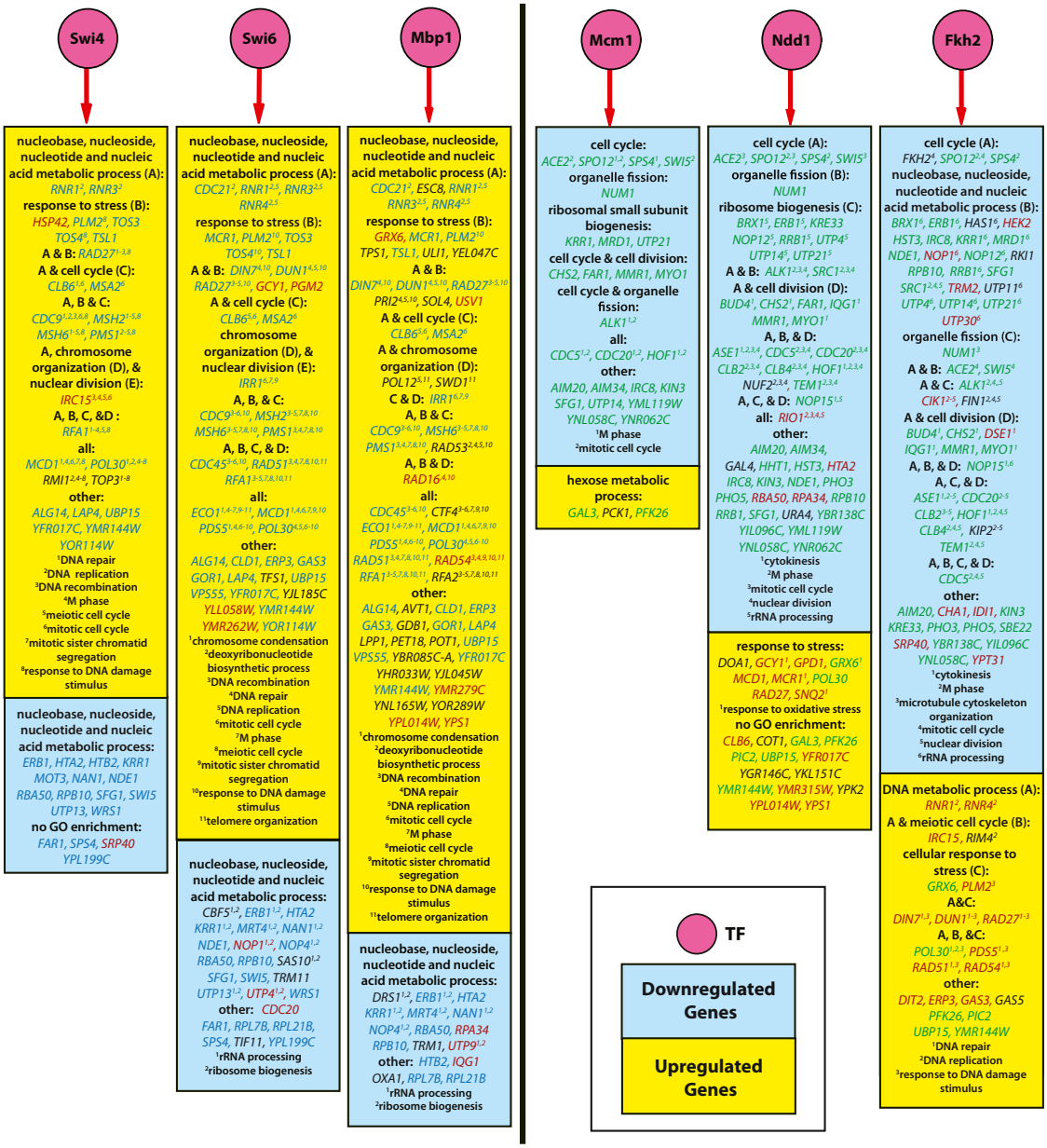

Figure S2. Network Diagram for Predicted Targets of Swi6, Swi4, Mbp1, Fkh2, Mcm1, and Ndd1, Related to Figure 3

All details are described in Figure S1. Genes in black are unique targets of the indicated TF, genes in blue are shared targets of components of either SBF (Swi6/Swi4) and/or MBF (Swi6/Mbp1), genes in green are shared targets of the Fkh2/Mcm1/Ndd1 complex, and genes in red are unique targets of the TF in the complex but shared with other TFs in Figure S1.

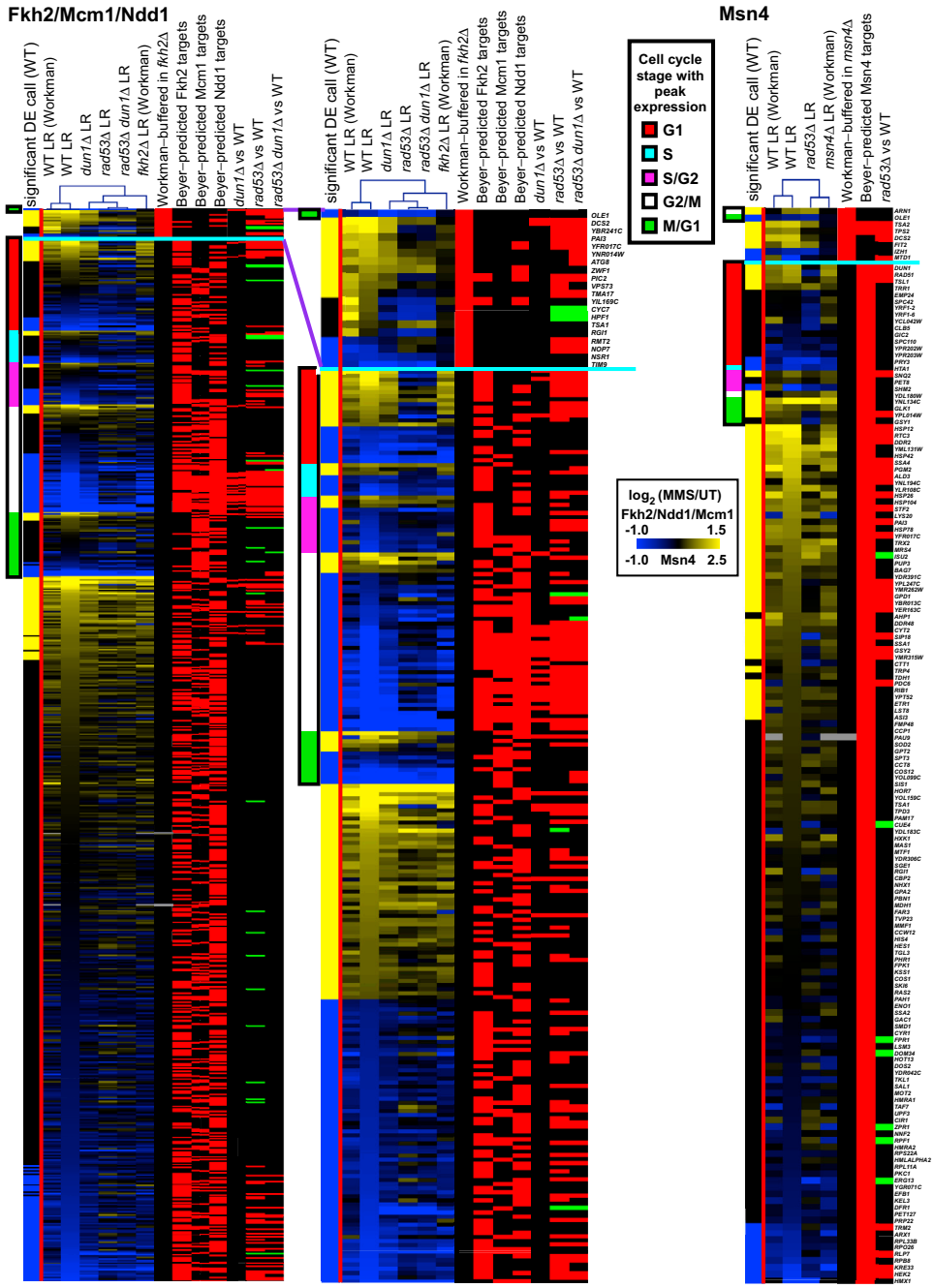

Figure S3. Heatmap of Fkh2/Mcm1/Ndd1 and Msn4 Target Gene Expression, Related to Figure 3

All potential targets of each TF from Beyer et al. are shown (Beyer et al., 2006). Also included above the light blue line are the genes that showed reduced differential expression (DE) in the *fkh2Δ* (heat map on the left) and *msn4Δ* (heat map on the right) mutants (Workman et al., 2006). The WT (DE) row indicates genes showing significant DE (upregulated genes in yellow and downregulated genes in blue) in response to MMS treatment in wild-type (WT). The degree of differential expression is also indicated by the intensity of blue (downregulated) or yellow (upregulated) color for the wild-type, *dun1*Δ (for Fkh2/Mcm1/Ndd1 targets), *rad53*Δ, and *dun1*Δ *rad53*Δ (for Fkh2/Mcm1/Ndd1 targets) strains generated in this study and for wild-type, *fkh2*Δ, and *msn4Δ* strains generated by Workman (Workman et al., 2006) The dendrograms at the top indicate clustering of the log ratios by Euclidean distance for all of the Fkh2-dependent (left) and Msn4-dependent (right) genes; profiles of both TFs cluster more closely to the *rad53*Δ strain, indicating that the majority of TF-dependent genes are kinase-dependent. Specific checkpoint kinase-dependent genes are indicated in the mutant versus WT row with red bars while genes with greater expression in the mutant are indicated with green bars. Color bars along the side mark genes with cell cycle-specific expression (Spellman et al., 1998). To simplify the Fkh2/Mcm1/Ndd1 diagram, the heat map in the middle zooms in specifically on genes with Fkh2-dependent DE (above the light blue line) and with significant DE in WT (below the blue line).

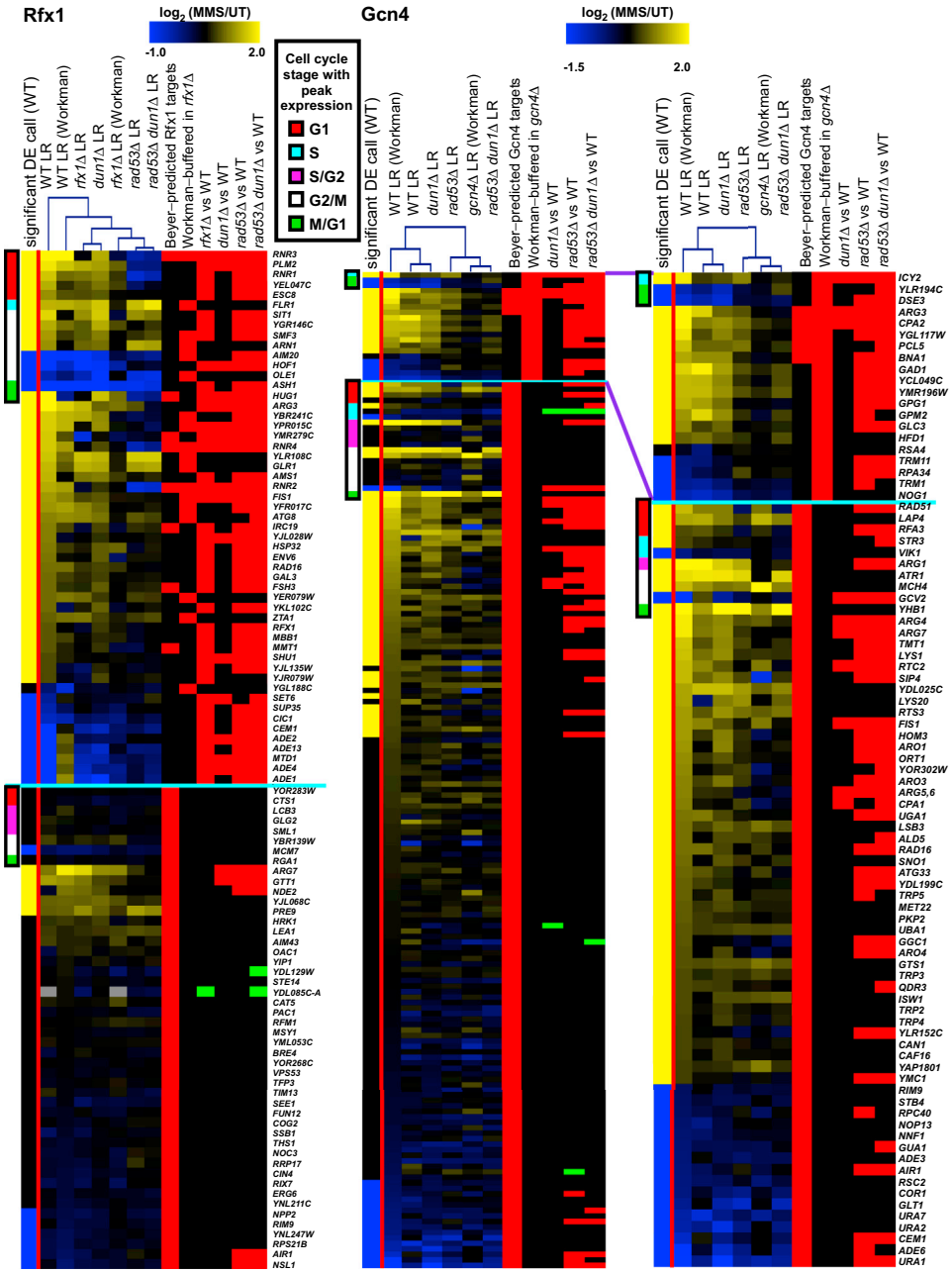

Figure S4. Heatmap of Rfx1 and Gcn4 Target Gene Expression, Related to Figure 3

All potential targets of each TF from Beyer et al. are shown (Beyer et al., 2006). Also included above the light blue line are the genes that showed reduced differential expression (DE) in the *rfx1Δ* (heat map on the left) and *gcn4Δ* (heat map on the right) mutants (Workman et al., 2006). The WT (DE) row indicates genes showing significant differential expression (upregulated genes in yellow and downregulated genes in blue) in response to MMS treatment in wild-type (WT). The degree of differential expression is also indicated by the intensity of blue (downregulated) or yellow (upregulated) color for the wild-type, *dun1*Δ, *rad53*Δ, and *dun1*Δ *rad53*Δ (and *rfx1*Δ for the Rfx1 heat map) strains generated in this study and for wild-type, *rfx1*Δ, and *gcn4Δ* strains generated by Workman (Workman et al., 2006). The dendrograms at the top indicate clustering of the log ratios by Euclidean distance for all Rfx1-dependent (left) and Gcn4-dependent (right) genes; profiles of both TFs cluster more closely to the *rad53*Δ strain, indicating that the majority of TF-dependent genes are kinase-dependent. Specific checkpoint kinase dependent genes are indicated in the mutant versus WT row with red bars while genes with greater expression in the mutant are indicated with green bars. Color bars along the side mark genes with cell cycle-specific expression (Spellman et al., 1998). To simplify the Gcn4 diagram, the heat map on the far right zooms in specifically on genes with Gcn4-dependent DE (above the light blue line) and with significant DE in WT (below the blue line).

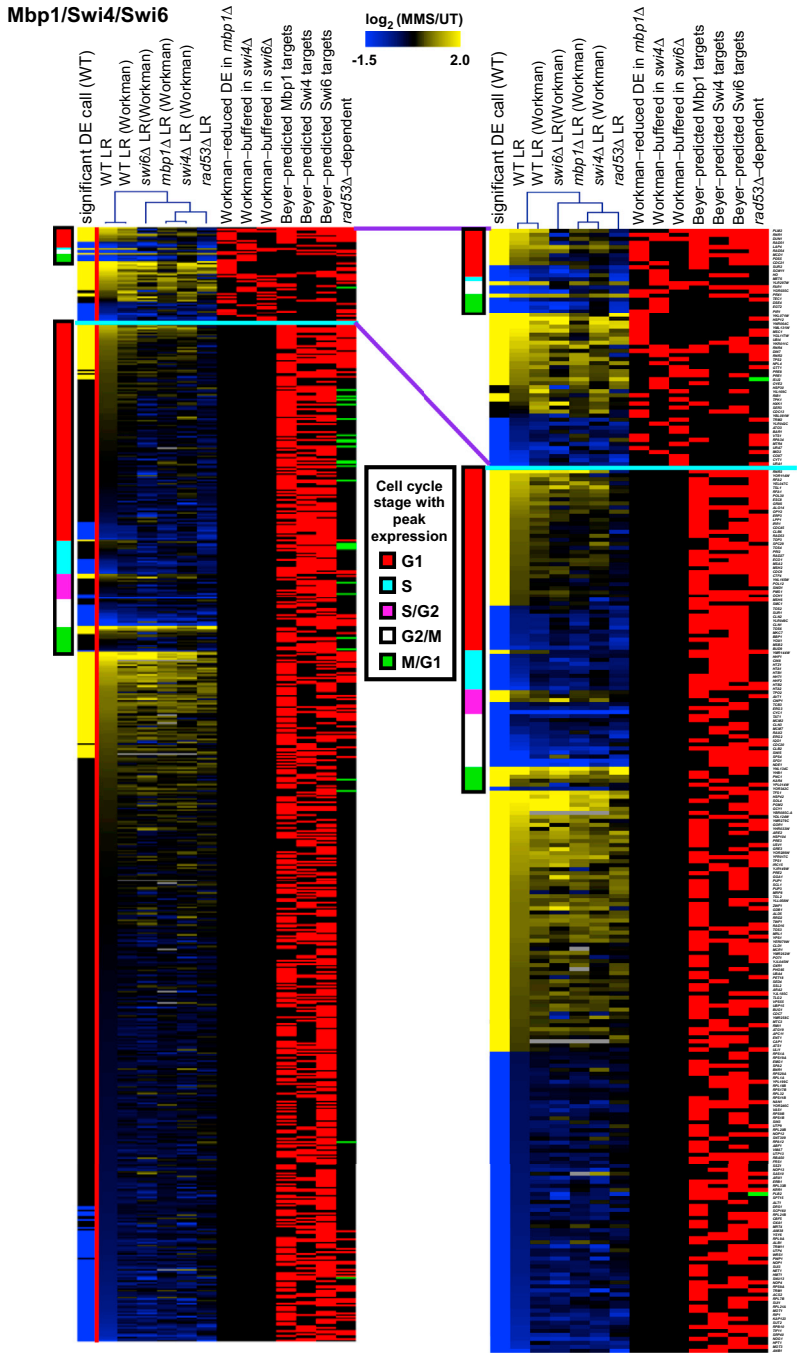

Figure S5. Heatmap of Mbp1, Swi4, and Swi6 Target Gene Expression, Related to Figure 3

All potential targets of each TF from Beyer et al. are shown (Beyer et al., 2006). Also included above the light blue line are the genes that showed reduced differential expression (DE) in the *mbp1Δ, swi4Δ,* and *swi6Δ* mutants (Workman et al., 2006). The WT (DE) row indicates genes showing significant DE (upregulated genes in yellow and downregulated genes in blue) in response to MMS treatment in wild-type (WT). The degree of differential expression is also indicated by the intensity of blue (downregulated) or yellow (upregulated) color for the wild-type and *rad53*Δ strains generated in this study and for wild-type, *mbp1Δ, swi4Δ,* and *swi6Δ* strains generated by Workman (Workman et al., 2006). The dendrograms at the top indicate clustering of the log ratios by Euclidean distance for the genes showing reduced DE in the *mbp1Δ, swi4Δ,* and *swi6Δ* strains; profiles of the three TFs cluster more closely to the *rad53*Δ strain, indicating that the majority of TF-dependent genes are kinase-dependent. Specific checkpoint kinase dependent genes are indicated in the mutant versus WT row with red bars while genes with greater expression in the mutant are indicated with green bars. Color bars at the top mark genes with cell cycle-specific expression (Spellman et al., 1998).To simplify the diagram, the heat map on the right zooms in on genes with Mbp1, Swi4, or Swi6-dependent DE (above the light blue line) and with significant DE in WT (below the blue line).

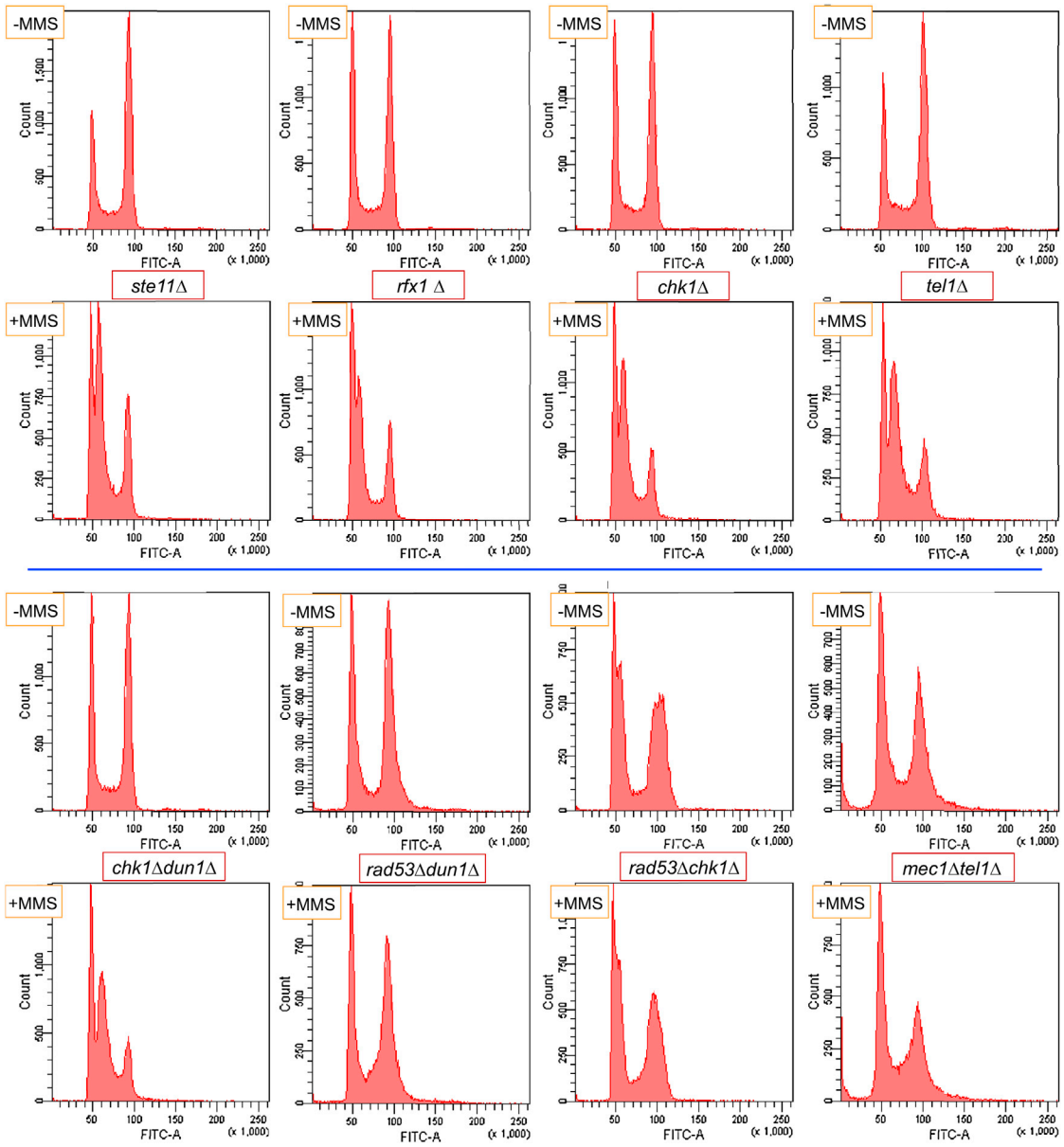

Figure S6. FACS Profiles for Checkpoint Kinase Defective Strains, Related to Figure 5

The data for all of the strains tested in the array experiments that are not included in Figure 5D are presented.

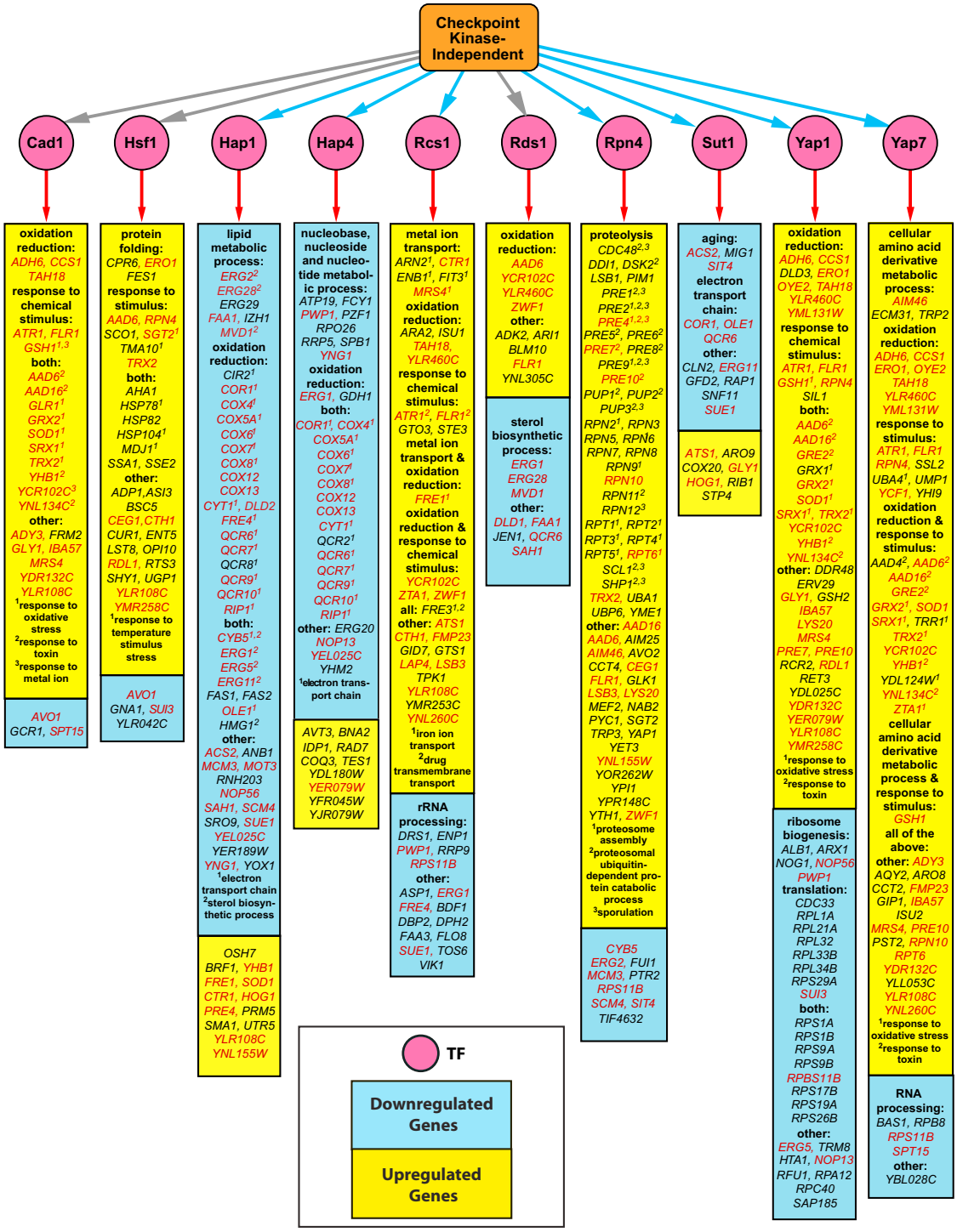

Figure S7. Network Diagram Showing the Checkpoint-Kinase-Independent TFs, Predicted Target Genes, and Noteworthy GO Terms Associated with Those Targets, Related to Figure 6

All TF target genes showing significant enrichment in the set of checkpoint kinase-independent genes (Figure 6A; Table S10) are included, grouped by associated GO terms from Table S7. Genes in black are unique targets of the TF, while genes in red are also targets of other TFs.

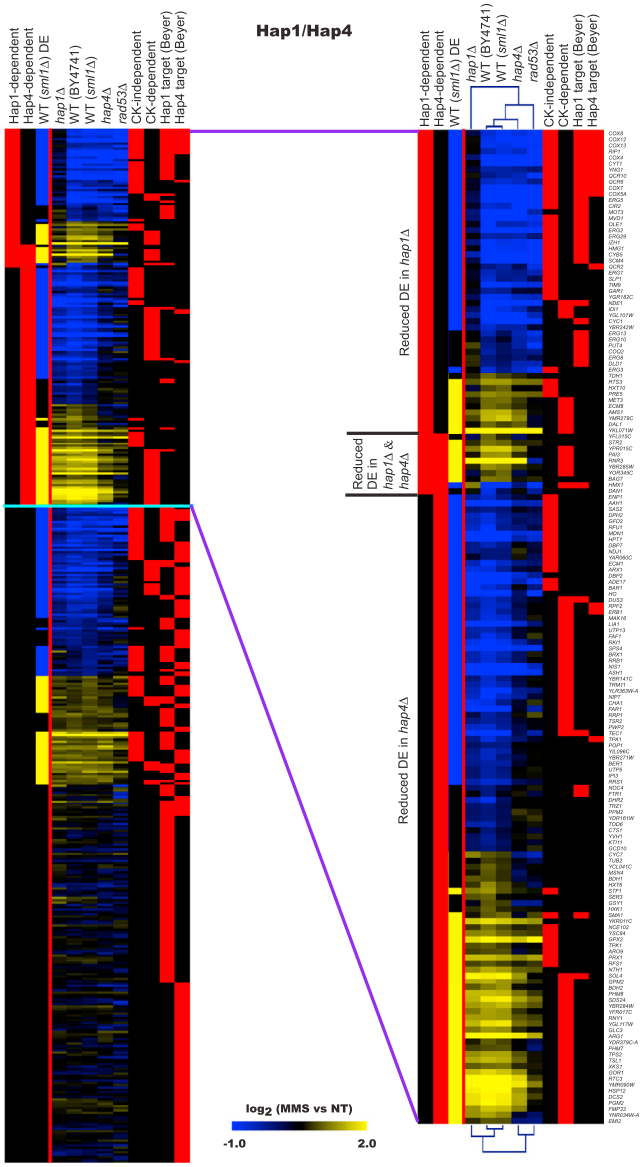

Figure S8. Heatmap of Hap1 and Hap4 Target Gene Expression, Related to Figure 6

All potential targets of Hap1 and Hap4 from Beyer et al. are shown (Beyer et al., 2006). Also included above the light blue line and in the panel on the right are the genes that showed reduced differential expression (DE) in the *hap1Δ* and *hap4Δ* mutants. The WT (DE) row indicates genes showing significant DE (upregulated genes in yellow and downregulated genes in blue) in response to MMS treatment in the wild-type (*sml1Δ*) sample from the checkpoint kinase mutant experiment. The degree of differential expression is indicated by the intensity of blue (downregulated) or yellow (upregulated) color for the wild-type (*sml1Δ*) and *rad53*Δ strains from the checkpoint kinase experiments and for the wild-type (BY4741), *hap1Δ*, and *hap4Δ* strains from the transcription factor experiments. Checkpoint kinase (CK)-independent and CK-dependent genes from the analysis described in Figure 6A and Table S10 are also indicated. The dendrogram at the top indicates clustering of the strains by Euclidean distance using log ratios of expression for all Hap1-dependent genes while the dendrogram at the bottom shows clustering analysis using the Hap4-dependent genes. While both the Hap1- and Hap4-dependent sets contain checkpoint kinase-independent genes, clustering the strains using Hap1-dependent genes indicates that those genes are primarily dependent on Hap1 but not Rad53 while clustering the strains using Hap4-dependent genes indicates that several Hap4-dependent genes are dependent on both Hap4 and Rad53.

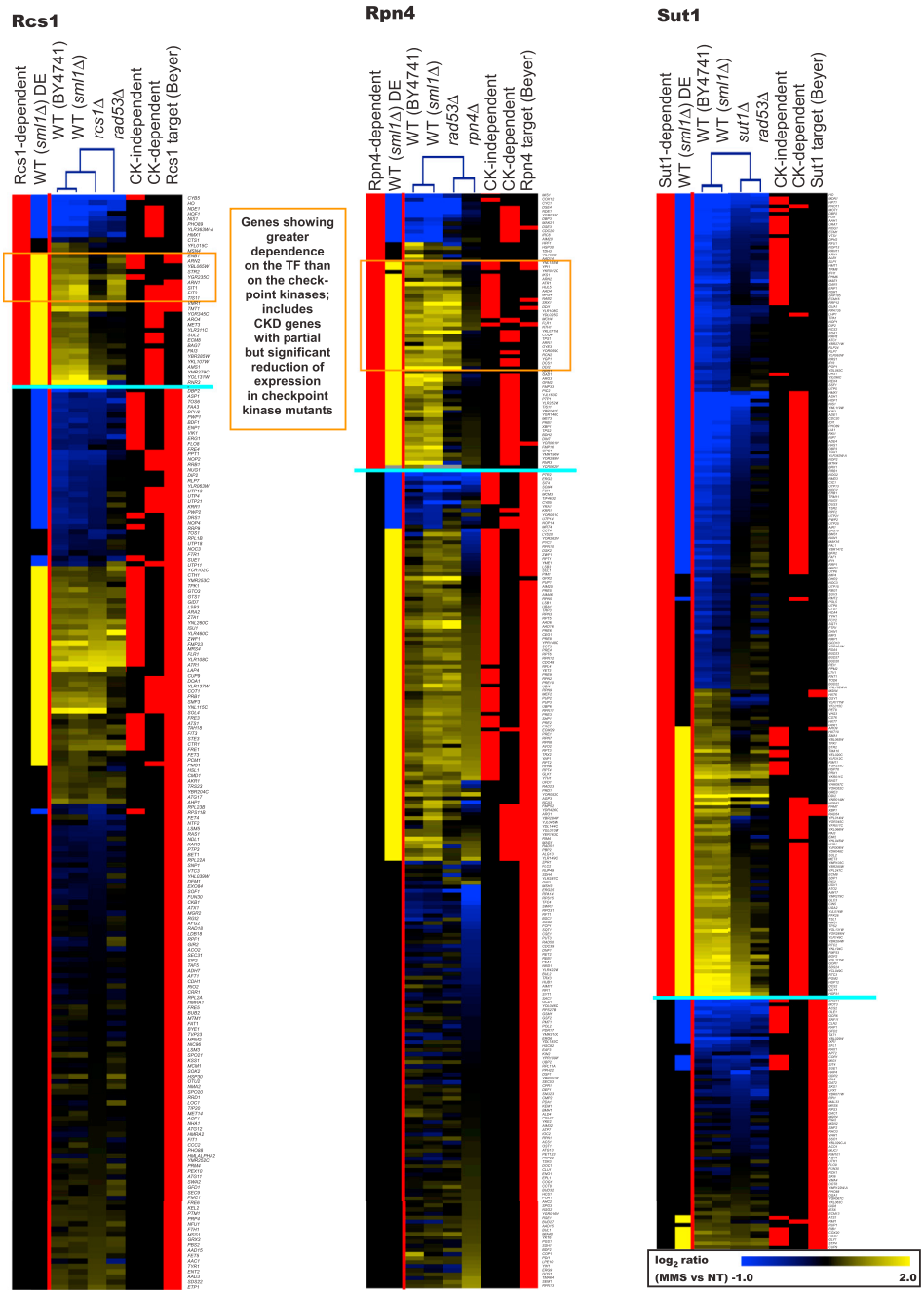

Figure S9. Heatmap of Rcs1, Rpn4, and Sut1 Target Gene Expression, Related to Figure 6

All potential targets of Rcs1 (left panel), Rpn4 (middle panel), and Sut1 (right panel) from Beyer et al. are shown (Beyer et al., 2006). Also included above the light blue lines are the genes that showed reduced differential expression (DE) in the *rcs1Δ* (left) and *sut1Δ* (right) mutants in our study and that were "buffered" by deletion of *RPN4* (middle) in the Workman study (Workman et al., 2006). The WT (DE) row indicates genes showing significant DE (upregulated genes in yellow and downregulated genes in blue) in response to MMS treatment in the wild-type (*sml1Δ*) sample from the checkpoint kinase mutant experiment. The degree of differential expression is indicated by the intensity of blue (downregulated) or yellow (upregulated) color for the wild-type (*sml1Δ*) and *rad53*Δ strains from the checkpoint kinase experiments and for the wild-type (BY4741), *rcs1Δ* (left), *rpn4Δ* (middle), and *sut1Δ* (right) strains from the transcription factor experiments performed here (Rcs1 and Sut1) or by Workman (Rpn4) (Workman et al., 2006). Checkpoint kinase (CK)-independent and CK-dependent genes from the analysis described in Figure 6A and Table S10 are also indicated. The dendrograms at the top indicate clustering of the strains by Euclidean distance using log ratios for expression of the respective TF-dependent genes. While the clustering analysis suggests that most of the TF-dependent genes are also Rad53-dependent, several CK-independent genes were observed in each set. Notably, both the Rcs1- and Rpn4-dependent gene sets include clusters of genes showing greater dependence on the TF than on Rad53 (orange boxes). Included in these clusters are genes classified as CK-dependent because deletion of the kinases results in partial but significant reduction in DE while deletion of the TF results in a more complete loss of DE.

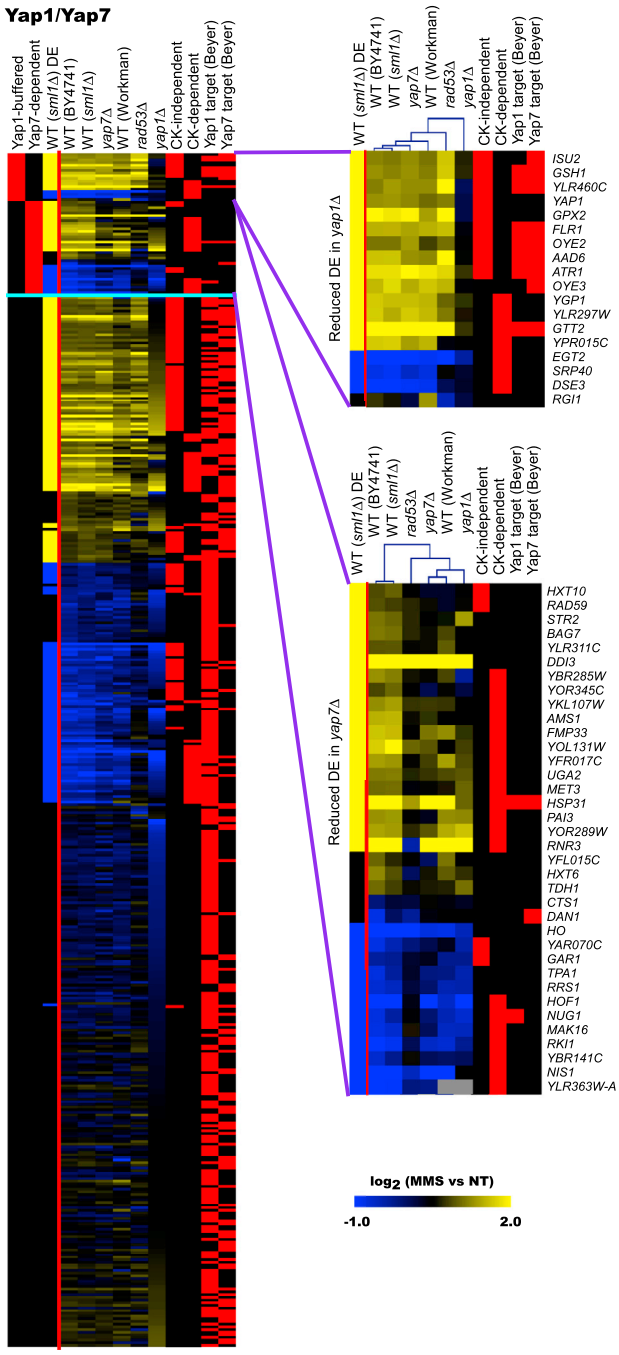

Figure S10. Heatmap of Yap1 and Yap7 Target Gene Expression, Related to Figure 6

All potential targets of Yap1 and Yap7 from Beyer et al. are shown (Beyer et al., 2006). Also included above the light blue line in the panel on left and shown in greater detail in the panels on the right are the genes that showed reduced differential expression (DE) in the *yap1Δ* (top right) and *yap7Δ* (bottom right) mutants. The WT (DE) row indicates genes showing significant DE (upregulated genes in yellow and downregulated genes in blue) in response to MMS treatment in the wild-type (*sml1Δ*) sample from the checkpoint kinase mutant experiment. The degree of differential expression is indicated by the intensity of blue (down-regulated) or yellow (upregulated) color for the wild-type (*sml1Δ*) and *rad53*Δ strains from the checkpoint kinase experiments and for the wild-type (BY4741), *yap1Δ*, and *yap7Δ* strains from the transcription factor experiments performed here (Yap7) or by Workman (Yap1) (Workman et al., 2006). Checkpoint kinase (CK)-independent and CK-dependent genes from the analysis described in Figure 6A and Table S10 are also indicated. The dendrograms in the panels on the right indicate clustering of the strains by Euclidean distance using the log ratios of all Yap1 (top) and Yap7 (bottom) dependent genes. While both the Yap1- and Yap7-dependent sets contain checkpoint kinase-independent genes, clustering the strains using Yap1-dependent genes indicates that those genes are primarily dependent on Yap1 but not Rad53 while clustering the strains using Yap7-dependent genes indicates that a large number of Yap7-dependent genes are dependent on both Yap7 and Rad53.